

# Neural Port-Hamiltonian Models for Nonlinear Distributed Control: An Unconstrained Parametrization Approach

Muhammad Zakwan and Giancarlo Ferrari-Trecate

**Abstract**—The control of large-scale cyber-physical systems requires optimal distributed policies relying solely on limited communication with neighboring agents. However, computing stabilizing controllers for nonlinear systems while optimizing complex costs remains a significant challenge. Neural Networks (NNs), known for their expressivity, can be leveraged to parametrize control policies that yield good performance. However, NNs’ sensitivity to small input changes poses a risk of destabilizing the closed-loop system. Many existing approaches enforce constraints on the controllers’ parameter space to guarantee closed-loop stability, leading to computationally expensive optimization procedures. To address these problems, we leverage the framework of port-Hamiltonian systems to design continuous-time distributed control policies for nonlinear systems that guarantee closed-loop stability and finite  $\mathcal{L}_2$  or incremental  $\mathcal{L}_2$  gains, independent of the optimization parameters of the controllers. This eliminates the need to constrain parameters during optimization, allowing the use of standard techniques such as gradient-based methods. Additionally, we discuss discretization schemes that preserve the dissipation properties of these controllers for implementation on embedded systems. The effectiveness of the proposed distributed controllers is demonstrated through consensus control of non-holonomic mobile robots subject to collision avoidance and averaged voltage regulation with weighted power sharing in DC microgrids.

## I. INTRODUCTION

Distributed control of *large-scale* systems presents significant challenges even in seemingly basic scenarios due to the constrained flow of information in real-time. Particularly, Witsenhausen’s counter-example [1] demonstrates that even under apparently ideal conditions (i.e. linear dynamics, quadratic loss, and Gaussian noise), a nonlinear distributed control policy can outperform the best linear one. The work [2] has provided necessary and sufficient condition, namely, Quadratic Invariance (QI), under which a distributed optimal controller is linear and can be designed by solving a convex optimization problem. However, real-world systems often violate the QI assumption due to inherent nonlinearities, non-convex control costs, or privacy limitations [3]. This necessitates venturing beyond linear control and exploring highly nonlinear distributed control policies, such as those parametrized by deep Neural Networks (NNs).

NNs have proved their capabilities in learning-enabled control [3]–[8], and system identification [9]–[14] of non-linear dynamical systems. Indeed, NN control has been applied in diverse contexts, such as robotics [4], epidemic models [15], safe path planning [6], and nonlinear consensus [16]. Existing

approaches to NN control design also include modelling the system under control as a NN from data [17]–[20]. Nevertheless, NNs can be susceptible to small changes in their inputs [21]. This fragility can readily lead to control policies jeopardizing closed-loop stability [11], thereby hindering their deployment in large-scale, safety-critical applications [6].

In this paper, we leverage the well-established port-Hamiltonian (pH) system framework [22] to provide an *unconstrained parametrization* of distributed control policies that are inherently endowed with a finite  $\mathcal{L}_2$  or an incremental  $\mathcal{L}_2$  ( $i\mathcal{L}_2$ ) gain. This allows casting optimal control design into an unconstrained optimization problem that can be solved using standard gradient-based methods such as stochastic gradient descent or its variants. As a consequence, our approach eliminates the need for computationally expensive procedures, such as the projection of parameters or constrained optimization techniques, which are typically required to guarantee closed-loop stability [6]. Specifically, if both the underlying system to be controlled and the proposed controller satisfy the conditions of the small-gain theorem [22], our framework can ensure closed-loop stability both during and after the training. Moreover, the learned distributed policies are optimal in the sense that they strive to minimize an arbitrary nonlinear cost function over a finite horizon.

**Related work:** NNs have shown promise in designing both static and dynamic distributed control policies for large-scale systems. Notably, Graph Neural Networks (GNNs) have achieved impressive performance in applications like vehicle flocking and formation flying [23]–[26] thanks to their inherent scalable structure. However, guaranteeing stability with general GNNs remains challenging, often requiring restrictive assumptions like linear, open-loop stable system dynamics or sufficiently small Lipschitz constants [26]. Such limitations can be impractical, potentially leading to system failures during the training phase before an optimal policy can be found [27], [28]. Some remedies to rectify this problem include improving an initial known safe policy iteratively, while imposing the constraint that the initial *region of attraction* does not shrink [29]–[31], and leveraging integral quadratic constraints to enforce the closed-loop stability [32]. However, these approaches explicitly constrain the optimization parameters of NNs, which may lead to infeasibility or hinder the closed-loop performance. In contrast, our proposed method based on unconstrained parametrizations provides the same scalability as GNNs without imposing any constraints on the optimization parameters to guarantee closed-loop stability. Previous works also explored stable-by-design control based on mechanical energy conservation [33], [34], but these methods are limited to specific systems (e.g., with SE(3) dynamics). Our approach, instead, applies to a much wider range of nonlinear systems.

This work was supported as a part of NCCR Automation, a National Centre of Competence in Research, funded by the Swiss National Science Foundation (grant number 51NF40\_225155)

Authors are with the Institute of Mechanical Engineering, Ecole Polytechnique Fédérale de Lausanne (EPFL), CH-1015 Lausanne, Switzerland {muhammad.zakwan}@epfl.ch

Recently, the notion of unconstrained parametrization has emerged for learning-enabled control, where a controller is parametrized such that it satisfy specific constraints (e.g., semi-definite constraints) *by design*, i.e. without being constrained. This allows one to bypass computationally expensive *a posteriori* verification routines. Based on this approach, the framework of Recurrent Equilibrium Networks (RENs) has been proposed in [11]. RENs are a class of discrete-time nonlinear dynamical models that enjoy built-in stability and robustness properties. Notably, subsets of RENs can satisfy desired integral quadratic constraints regardless of their optimization parameters and ensure a finite  $\mathcal{L}_2$  gain. Despite their flexibility, RENs face some key limitations. Firstly, they consider dynamics that are dissipative with respect to quadratic storage functions, potentially limiting their expressiveness for complex systems. Secondly, the unconstrained parametrization approach in [11], [35] cannot be directly applied to distributed systems where sparsity patterns in weight matrices are crucial. In contrast, our framework based on pH models allows the use of arbitrary nonlinear storage functions to capture more complex dynamics. Additionally, it seamlessly integrates desired sparsity patterns into the optimization parameters, enhancing flexibility without compromising stability. Since our framework is based on pH systems, a limitation of our controllers is that they have the same number of inputs and outputs. This is not required for RENs. Building on RENs, the work [36] presents an unconstrained parametrization approach for interconnecting subsystems with finite  $\mathcal{L}_2$  gain, while guaranteeing the  $\mathcal{L}_2$  stability of the overall system. However, this approach is limited to quadratic storage functions for subsystems, constraining flexibility and generalization. The work [3] presented a distributed framework based on pH systems that ensure passivity by design. However, it assumes that subsystems are in the pH form as well. Moreover, it does not guarantee finite  $\mathcal{L}_2$  or  $i\mathcal{L}_2$  gains for the closed-loop system which is instead our main result. Unlike passivity, a finite  $\mathcal{L}_2$  gain guarantees stability even in the presence of external disturbances or modeling errors, which is crucial for safe operation in uncertain environments [22], [37].

**Contributions:** The main contributions of this paper can be summarized as follows:

- 1) We provide an unconstrained parametrization of a class of distributed controllers in the pH form that can seamlessly incorporate sparsity in their weight matrices and are inherently endowed with a finite  $\mathcal{L}_2$  or  $i\mathcal{L}_2$  gain.
- 2) Our approach overcomes the limitation of being restricted to specific storage functions (e.g., quadratic), enabling its application to a broader range of nonlinear control problems.
- 3) We illustrate how discrete gradient methods [38] can be leveraged to preserve the dissipative properties when continuous-time pH controllers are discretized in time for implementation purposes.
- 4) We demonstrate the effectiveness of our controllers on a benchmark consensus problem for non-holonomic agents subject to a collision avoidance constraint, and weighted power sharing and average voltage regulation

in DC microgrids.

**Organization:** Section II presents the problem formulation. We then introduce unconstrained parametrizations of distributed controllers using pH models that guarantee a finite  $\mathcal{L}_2$  gain (Section III), or a finite  $i\mathcal{L}_2$  gain (Section IV). Moreover, Section V discusses the discretization methods to preserve these gains for practical implementation. Finally, the performance evaluation of our proposed pH controllers is presented in Section VI, while Section VII concludes the paper.

A preliminary version of this work appeared in [39], which is, however, substantially different from the present paper. Indeed, the following results were not provided: (i) the unconstrained parametrization of a finite  $i\mathcal{L}_2$  gain (ii) the use of dissipation-preserving discretization schemes for implementation purposes, and (iii) a detailed proof of the unconstrained parametrization of pH models with finite  $\mathcal{L}_2$  gains.

**General notation:** The set of non-negative real numbers is  $\mathbb{R}_+$  and the standard Euclidean 2-norm is denoted by  $\|\cdot\|$ . The identity matrix of size  $n$  is denoted by  $I_n$ , a zero/null matrix of dimension  $n \times m$  is given by  $0_{n \times m}$ , and  $\mathbb{1}$  is a vector of all ones with an appropriate dimension. The maximal eigenvalue of a matrix  $A$  is represented by  $\bar{\lambda}(A)$ . We represent the set of  $\mathbb{R}^n$ -valued Lebesgue square-integrable functions by  $\mathcal{L}_2^n := \{v : [0, \infty) \rightarrow \mathbb{R}^n \mid \|v\|_2^2 := \int_0^\infty v(t)^\top v(t) dt < \infty\}$ . We omit the dimension  $n$  whenever it is clear from the context. Then, for any two  $v, w \in \mathcal{L}_2^n$ , we denote the  $\mathcal{L}_2^n$ -inner product as  $\langle v, w \rangle := \int_0^\infty v(t)^\top w(t) dt$ . Define the truncation operator  $(P_{\mathcal{T}}v)(t) := v(t)$  for  $t \leq \mathcal{T}$ ;  $(P_{\mathcal{T}}v)(t) := 0$  for  $t > \mathcal{T}$ , and the extended function space  $\mathcal{L}_{2e}^n := \{v : [0, \infty) \rightarrow \mathbb{R}^n \mid P_{\mathcal{T}}v \in \mathcal{L}_2, \forall \mathcal{T} \in [0, \infty)\}$ . For any linear space  $\mathcal{U}$  endowed with a norm  $\|\cdot\|_{\mathcal{U}}$ , we define a Banach space  $\mathcal{L}_{2e}(\mathcal{U})$  that consists of all measurable functions  $f : \mathbb{R}_+ \mapsto \mathcal{U}$  such that  $\int_0^\infty \|f(t)\|_{\mathcal{U}}^2 dt < \infty$ . Throughout this paper, a system will be specified by an input–output map  $\Sigma : \mathcal{L}_{2e}^m \rightarrow \mathcal{L}_{2e}^p$  satisfying  $\Sigma(0) = 0$ . Given two systems  $\Sigma_1$  and  $\Sigma_2$ , the standard negative feedback configuration between them is denoted by  $\Sigma_1 \parallel_f \Sigma_2$ , see Fig. 2. Let  $\mathcal{G} = (\mathcal{V}, \mathcal{E})$  be an undirected graph with nodes  $\mathcal{V} = \{1, \dots, N\}$  and edges  $\mathcal{E}$ , and let  $\mathcal{P} \in \{0, 1\}^{N \times N}$  be the corresponding adjacency matrix. For a binary mask  $\mathcal{M} \in \{0, 1\}^{m \times n}$ , we denote  $\mathbf{W} \in \text{blkSparse}(\mathcal{M})$  if  $\mathbf{W}$  is a block matrix composed by  $m \times m$  blocks and  $\mathcal{M}_{i,j} = 0 \Rightarrow \mathbf{W}_{i,j} = 0$ .  $\mathbf{A} = \text{blkdiag}(A_i)$  represents a block-diagonal matrix with matrices  $A_0, A_1, \dots, A_i$  on the diagonal.

**Preliminaries:** Consider the following non-linear system

$$\Sigma : \begin{cases} \dot{x}(t) = f(x(t), u(t)), \\ y(t) = h(x(t)), \end{cases} \quad (1a) \quad (1b)$$

where  $x \in \mathcal{X} \subseteq \mathbb{R}^n$  is the state,  $u \in \mathcal{U} \subseteq \mathbb{R}^m$  is the input, and  $y \in \mathcal{Y} \subseteq \mathbb{R}^p$  is the output of the system  $\Sigma$ . Moreover, assume there exists a unique solution  $x(t)$  on the infinite time interval  $[0, \infty)$  of (3a) for all initial conditions  $x(0) \in \mathcal{X}$ , and  $u(\cdot) \in \mathcal{L}_{2e}(\mathcal{U})$ . We recall some important results and definitions that are used to obtain the main results of this paper.

*Definition 1 (Dissipativity, [22]):* The system  $\Sigma$  is called dissipative w.r.t. to a supply rate  $s : \mathcal{U} \times \mathcal{Y} \mapsto \mathbb{R}$ , if there exists a smooth storage function  $V : \mathcal{X} \mapsto \mathbb{R}_+^1$  such that

$$\dot{V}(x(t)) \leq s(u(t), y(t)), \quad \forall t \in \mathbb{R}_+,$$

or equivalently,

$$V(x(\tau)) - V(x(0)) \leq \int_0^\tau s_i(u(t), y(t)) dt,$$

for every input signal  $u(t) \in \mathcal{U}$ , output signal  $y(t) \in \mathcal{Y}$  and  $\tau \geq 0$ . Moreover, the choice of the supply rate leads to different notions of dissipativity, for instance,

- if  $p = m$ , and  $s(u(t), y(t)) = u(t)^\top y(t)$ , then system  $\Sigma$  is passive;
- if  $p = m$ , and  $s(u(t), y(t)) = u(t)^\top y(t) - \epsilon \|y(t)\|$ , then system  $\Sigma$  is  $\epsilon$ -output strictly passive for  $\epsilon > 0$ ;
- for some non-negative constants  $\gamma, b$ , if  $s(u(t), y(t)) = \frac{\gamma^2}{2} \|u(t)\| - \frac{1}{2} \|y(t)\|$ , then system  $\Sigma$  has a finite  $\mathcal{L}_2$  gain, i.e.  $\|y(t)\| \leq \gamma \|u(t)\| + b$ .

Consider the interconnection  $\Sigma_1 \parallel_f \Sigma_2$  of two dissipative systems  $\Sigma_1$ , and  $\Sigma_2$  in Fig. 2. Then, one can leverage the following result to ensure closed-loop stability.

*Theorem 1 ([22]):* Consider the closed-loop system  $\Sigma_1 \parallel_f \Sigma_2$  given in Fig. 2.

- (small gain condition) Assume the existence of the  $\mathcal{L}_2$  gains  $\mathcal{L}_2(\Sigma_1) \leq \gamma_1$ , and  $\mathcal{L}_2(\Sigma_2) \leq \gamma_2$ . Then, the closed-loop system  $\Sigma_1 \parallel_f \Sigma_2$  is stable with an  $\mathcal{L}_2$  gain  $\gamma_1 \cdot \gamma_2$  if  $\gamma_1 \cdot \gamma_2 < 1$ ;
- (strict output passivity) Assume that, for any  $e_1 \in \mathcal{L}_{2e}(\mathcal{U}_1)$  and  $e_2 = 0$ ,  $\Sigma_1 : \mathcal{L}_{2e}(\mathcal{U}_1) \rightarrow \mathcal{L}_{2e}(\mathcal{Y}_1)$  is  $\epsilon_1$ -output strictly passive, and  $\Sigma_2 : \mathcal{L}_{2e}(\mathcal{U}_2) \rightarrow \mathcal{L}_{2e}(\mathcal{Y}_2)$  is passive. Then for  $e_2 = 0$ ,  $\Sigma_1 \parallel_f \Sigma_2$  with input  $e_1$  and output  $y_1$  has an  $\mathcal{L}_2$ -gain  $\leq 1/\epsilon_1$ .

We recall that  $\epsilon$ -output strict passivity also implies a finite  $\mathcal{L}_2$  gain not larger than  $1/\epsilon$  [22].

While Theorem 1 guarantees  $\mathcal{L}_2$  stability of the closed-loop system, in several cases a stronger notion of stability, such as a finite  $i\mathcal{L}_2$  gain, is required [22]. Incremental stability [40] has garnered increasing interest in recent years due to its potential applications in the synchronization of chaotic systems [41], [42] and nonlinear circuits [43]. Moreover, incremental  $\mathcal{L}_2$  stability implies that any two trajectories must eventually asymptotically converge to each other, regardless of their initial conditions [44]. Since incremental stability is an incremental dissipativity property, we formally recall the latter notion.

*Definition 2 (Incremental Dissipativity, [45]):*

The system  $\Sigma$  is called incrementally dissipative w.r.t. to a supply rate  $s_\Delta : \mathcal{U} \times \mathcal{U} \times \mathcal{Y} \times \mathcal{Y} \mapsto \mathbb{R}$ , if there exists a smooth storage function  $V_\Delta : \mathcal{X} \times \mathcal{X} \mapsto \mathbb{R}_+$  such that for any two trajectories  $(x, u, y), (\tilde{x}, \tilde{u}, \tilde{y})$

$$\dot{V}_\Delta(x(t), \tilde{x}(t)) \leq s_\Delta(u(t), \tilde{u}(t), y(t), \tilde{y}(t)), \quad \forall t \in \mathbb{R}_+,$$

<sup>1</sup>For  $\mathcal{X} = \mathbb{R}^n$ , the storage function has to be radially unbounded, that is  $V(x) \rightarrow \infty$ , whenever  $\|x\| \rightarrow \infty$  [22, Theorem 3.2.4].

or equivalently,

$$\begin{aligned} V_\Delta(x(\tau), \tilde{x}(\tau)) - V_\Delta(x(0), \tilde{x}(0)) \\ \leq \int_0^\tau s_\Delta(u(t), \tilde{u}(t), y(t), \tilde{y}(t)) dt, \end{aligned}$$

for every pair of input signals  $u(t), \tilde{u}(t) \in \mathcal{U}$ , output signals  $y(t), \tilde{y}(t) \in \mathcal{Y}$  and every  $\tau \geq 0$ . Moreover, the choice of supply rate leads to different notions of dissipativity, for instance,

- if  $p = m$ , and  $s_\Delta(u(t), \tilde{u}(t), y(t), \tilde{y}(t)) = (u(t) - \tilde{u}(t))^\top (y(t) - \tilde{y}(t))$ , then system  $\Sigma_s$  is incrementally passive;
- if  $p = m$ , and  $s_\Delta(u(t), \tilde{u}(t), y(t), \tilde{y}(t)) = (u(t) - \tilde{u}(t))^\top (y(t) - \tilde{y}(t)) - \epsilon_\Delta \|y(t) - \tilde{y}(t)\|$ , then system  $\Sigma$  is  $\epsilon_\Delta$ -output strictly incrementally passive for  $\epsilon_\Delta > 0$ ;
- if  $s_\Delta(u(t), \tilde{u}(t), y(t), \tilde{y}(t)) = \gamma_\Delta^2 \|u(t) - \tilde{u}(t)\| - \|y(t) - \tilde{y}(t)\|$ , then system  $\Sigma$  has a finite  $i\mathcal{L}_2$  gain, i.e.  $\|y(t) - \tilde{y}(t)\| \leq \gamma_\Delta \|u(t) - \tilde{u}(t)\|$  for a non-negative constant  $\gamma_\Delta$ , which is called the incremental gain.

Note that  $\epsilon_\Delta$ -output strictly incremental passivity implies an  $i\mathcal{L}_2$  gain of  $1/\epsilon_\Delta$  [22, Proposition 2.2.22]. The following result about closed-loop properties parallels Theorem 1.

*Theorem 2 ([22]):* Consider the closed-loop system  $\Sigma_1 \parallel_f \Sigma_2$  given in Fig. 2.

- (incremental form of small gain condition) Assume the existence of the  $i\mathcal{L}_2$  gains  $\mathcal{L}_2^\Delta(\Sigma_1) \leq \gamma_{\Delta,1}$ , and  $\mathcal{L}_2^\Delta(\Sigma_2) \leq \gamma_{\Delta,2}$ . Then, the closed-loop system  $\Sigma_1 \parallel_f \Sigma_2$  is stable with an  $i\mathcal{L}_2$  gain  $\gamma_{\Delta,1} \cdot \gamma_{\Delta,2} < 1$ ;
- (strict output incremental passivity) Assume that, for any  $e_1 \in \mathcal{L}_{2e}(\mathcal{U}_1)$  and  $e_2 = 0$ ,  $\Sigma_1 : \mathcal{L}_{2e}(\mathcal{U}_1) \rightarrow \mathcal{L}_{2e}(\mathcal{Y}_1)$  is  $\epsilon_{\Delta,1}$ -output strictly passive, and  $\Sigma_2 : \mathcal{L}_{2e}(\mathcal{U}_2) \rightarrow \mathcal{L}_{2e}(\mathcal{Y}_2)$  is incrementally passive. Then,  $\Sigma_1 \parallel_f \Sigma_2$  for  $e_2 = 0$  with input  $e_1$  and output  $y_1$  has an  $i\mathcal{L}_2$ -gain  $\leq 1/\epsilon_{\Delta,1}$ .

The conditions provided in Definition 2 for ensuring a finite  $i\mathcal{L}_2$  gain lead to Hamilton-Jacobi inequalities, which are nonlinear infinite-dimensional partial differential constraints that are difficult to satisfy [22]. Another approach, used in this paper, is to analyze the infinitesimal variation in the trajectories, as done in contraction theory [45]. To this end, we introduce the notion of differential dissipativity.

*Definition 3 (Differential Dissipativity, [45]):*

Consider the system  $\Sigma$  and its variational dynamics

$$\Sigma_\delta : \begin{cases} \delta \dot{x} = A(x, \delta x) \delta x + B(x, \delta x) \delta u, \\ \delta y = C(x, \delta x) \delta x, \end{cases}$$

where  $A(x, \delta x) := \frac{\partial}{\partial x} f(x, u)$ ,  $B(x, \delta x) := \frac{\partial}{\partial u} f(x, u)$ ,  $C(x, \delta x) := \frac{\partial}{\partial x} h(x)$  are matrix-valued functions. Then,  $\Sigma$  and  $\Sigma_\delta$  are called differentially dissipative w.r.t. to the supply function  $s_\delta : \mathcal{U} \times \mathcal{Y} \rightarrow \mathbb{R}$ , if there exists a smooth storage function  $V_\delta : \mathcal{X} \times \mathcal{X} \rightarrow \mathbb{R}^+$ , with  $V_\delta(\cdot, 0) = 0$  such that

$$\begin{aligned} V_\delta(x(t_1), \delta x(t_1)) - V_\delta(x(t_0), \delta x(t_0)) \\ \leq \int_{t_0}^{t_1} s_\delta(\delta u(t), \delta y(t)) dt \end{aligned}$$

for all  $t_0, t_1 \in \mathbb{R}$  with  $t_0 \leq t_1$  and for all  $(\delta x, \delta u)$ .

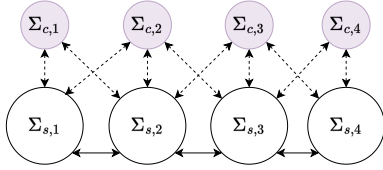


Fig. 1: An example of an interconnected system  $\Sigma_s$  and a distributed controller  $\Sigma_c$  for  $N = 4$ . The solid lines represent interactions between the subsystems of  $\Sigma_s$ , and the dashed lines represent the flow of information between the system  $\Sigma_s$  and the controller  $\Sigma_c$ .

## II. PROBLEM FORMULATION

In this section, we formally formulate the distributed control problem of interest. To this end, we consider a network  $\Sigma_s$  of  $N$  coupled nonlinear subsystems, each endowed with a feedback control policy. Let  $\mathcal{G}_s = (\mathcal{V}_s, \mathcal{E}_s)$  represent the undirected graph associated with the couplings among subsystems, and let  $\mathcal{P}_s$  be its corresponding adjacency matrix. We assume each subsystem is governed by

$$\Sigma_{s,i} : \begin{cases} \dot{x}_i(t) = f_i(x_i(t), \check{x}_i(t), u_i(t)), \\ y_i(t) = h_i(x_i(t)), \end{cases} \quad \forall i \in \mathcal{V}_s, \quad (3a)$$

$$(3b)$$

where  $x_i \in \mathcal{X}_i \subseteq \mathbb{R}^{n_i}$  is the state,  $u_i \in \mathcal{U}_i \subseteq \mathbb{R}^{m_i}$  is the input, and  $y_i \in \mathcal{Y}_i \subseteq \mathbb{R}^{p_i}$  is the output of the subsystem  $\Sigma_{s,i}$ , respectively.<sup>2</sup> We define  $\check{x}_i$  as a stacked vector of states of the 1-hop neighbors of subsystem  $i$  according to  $\mathcal{G}_s$ , i.e. all subsystems that influence  $x_i$ . Moreover, we assume there exists a unique solution trajectory on the infinite time interval  $[0, \infty)$  of (3a) for all initial conditions  $x_i(0) \in \mathcal{X}_i$ , and  $u_i(\cdot) \in \mathcal{L}_2(\mathcal{U}_i)$ .

The distributed control of large-scale systems presents a major challenge: local controllers at each subsystem  $u_i(t)$  can only access real-time information from a limited set of neighbors, dictated by a communication network, which is modeled as an undirected graph  $\mathcal{G}_c = (\mathcal{V}_c, \mathcal{E}_c)$ . This network is equivalently represented by the adjacency matrix  $\mathcal{P}_c \in \{0, 1\}^{N \times N}$ , where  $\mathcal{P}_{c_{i,i}} = 1$  for every  $i \in \mathcal{V}_c$ . In this paper, our goal is to develop distributed dynamic feedback controller  $\Sigma_c$  represented by the pairs  $(\chi_i(\cdot), \pi_i(\cdot)), i \in \mathcal{V}_c$  defining local controllers with some parameters  $\theta_i \in \mathbb{R}^{d_i}$

$$\Sigma_{c,i} : \begin{cases} \dot{\xi}_i(t) = \chi_i(\xi_i(t), \check{y}_i(t), \theta_i), & \xi_i \in \Xi_i \subseteq \mathbb{R}^{q_i}, \\ u_i(t) = \pi_i(\xi_i(t), \check{y}_i(t), \theta_i), \end{cases} \quad (4)$$

where  $\xi_i$  is the state of  $\Sigma_{c,i}$ , and  $\check{y}_i(t)$  is a stacked vector of outputs from the neighboring subsystems based on the communication graph  $\mathcal{G}_c$ . An example of a communication graph between the distributed controller  $\Sigma_c$  and the distributed system  $\Sigma_s$  is shown in Fig. 1.

Particularly, in this paper, we are interested in controllers  $\Sigma_{c,i}$  that are dissipative, endowed with some finite  $\mathcal{L}_2$  or  $i\mathcal{L}_2$  gains, and admit an *unconstrained parametrization*, i.e. for a given  $\gamma(\gamma_\Delta) > 0$ ,

$$\Sigma_{c,i} \text{ has finite } \mathcal{L}_2 \text{ (} i\mathcal{L}_2 \text{) gain } \gamma \text{ (} \gamma_\Delta \text{) for all } \theta_i \in \mathbb{R}^{d_i}. \quad (5)$$

<sup>2</sup>The sets  $\mathcal{X}_i, \mathcal{U}_i$ , and  $\mathcal{Y}_i$  are assumed to be non-empty.

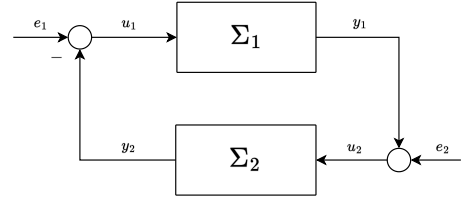


Fig. 2: Standard feedback interconnection  $\Sigma_1 \parallel_f \Sigma_2$ .

The term “unconstrained” refers to the fact that prescribed bounds on the  $\mathcal{L}_2$  ( $i\mathcal{L}_2$ ) gains, i.e. the property (5) must be guaranteed irrespectively of the value of  $\theta_i \in \mathbb{R}^{d_i}$ . In fact, the main result of this paper is to use pH systems for defining sets of controllers verifying (5). We define  $\theta = (\theta_1, \dots, \theta_N)$ . Moreover, the control policies  $\Sigma_c$  should be *optimal* in the sense that they minimize an arbitrary real-valued cost function

$$c(\mathbf{x}(t), \mathbf{u}(t)) = \frac{1}{T} \int_0^T \ell(\mathbf{x}(t), \mathbf{u}(t)) dt \quad (6)$$

for a finite horizon  $T \in \mathbb{R}_+$ , where  $c$  is differentiable almost everywhere. The bold-faced signals  $\mathbf{x}(t) = [x_1^\top, \dots, x_N^\top]^\top$ ,  $\mathbf{u}(t) = [u_1^\top, \dots, u_N^\top]^\top$  represent concatenated local states and local inputs, respectively.

Besides designing optimal control policies, ensuring the stability of the closed-loop system  $\Sigma_s \parallel_f \Sigma_c$  is equally crucial. To address this issue, in the remainder of this paper, we focus on achieving several notions of closed-loop stability, such as  $\mathcal{L}_2$  or  $i\mathcal{L}_2$  stability based on the small-gain theorem, or strictly output passivity (Theorem 1, and 2). In a nutshell, these conditions enforce a prescribed  $\mathcal{L}_2$  or  $i\mathcal{L}_2$  gain on the controller  $\Sigma_c$  for guaranteeing closed-loop stability.

The overall problem can be formulated as the following Optimal Control Problem (OCP)

$$\begin{aligned} \min_{\theta} \quad & \frac{1}{S} \sum_{k=1}^S c(\mathbf{x}, \mathbf{u}; \theta, \mathbf{x}_0^k, \xi_0^k) \\ \text{s.t.} \quad & \text{system dynamics } \Sigma_s \\ & \text{controller dynamics } \Sigma_c \\ & \Sigma_c \text{ has a prescribed finite } \mathcal{L}_2, \\ & \text{or } i\mathcal{L}_2 \text{ gain, } \forall \theta \in \mathbb{R}^d, \end{aligned} \quad (7)$$

where  $\mathbf{x}_0^k, \xi_0^k, k = 1, \dots, S$  are samples of initial conditions for  $\Sigma_s$ , and  $\Sigma_c$ , respectively.<sup>3</sup>

*Remark 1 (Time-varying parameters):* In several applications of nonlinear OCP, time-varying optimization parameters provide additional degrees of freedom to minimize an arbitrary cost function during a transient time over a finite horizon  $T$ . For instance, a mechanical robot performs some complex maneuvers for a finite time and then asymptotically reaches an equilibrium point. Therefore, one can choose a time-varying parametrization as follows:

$$\theta(t) = \begin{cases} \theta(t) & \text{for } t \in [0, T], \\ \theta(T) & \text{for } t > T, \end{cases}$$

<sup>3</sup>Note that the empirical average in the cost is an approximation of the exact and often uncomputable average  $\mathbb{E}_{\mathbf{x}_0 \in \Omega_s, \xi_0 \in \Omega_c} [c(\mathbf{x}, \mathbf{u}; \theta, \mathbf{x}_0, \xi_0)]$  defined w.r.t. a probability distribution over the initial conditions.

where the optimization parameters  $\theta(T)$  are frozen for  $t > T$  and are computed such that  $\Sigma_c$  has a finite  $\mathcal{L}_2$ , or incremental  $\mathcal{L}_2$  gain. We demonstrate the efficacy of using time-varying weights by showing the consensus of non-holonomic agents in Section VI-A.

#### A. Port-Hamiltonian controllers

We consider local controllers (4) in the form

$$\Sigma_{pH,i} : \begin{cases} \dot{\xi}_i(t) = [J_i - (\alpha I + \Lambda_i)] \frac{\partial H_i}{\partial \xi_i}(\xi_i, \vartheta_i) + G_i \check{y}_i(t) \\ u_i(t) = G_i^\top \frac{\partial H_i}{\partial \xi_i}(\xi_i, \vartheta_i), \quad \forall i \in \mathcal{V}_s, \end{cases} \quad (9)$$

where the interconnection matrix  $J_i = -J_i^\top$  is skew-symmetric, and the damping is determined by a diagonal matrix  $(\alpha I_{q_i} + \Lambda_i) > 0$ , where  $\alpha > 0$  is a constant, and  $\Lambda_i := \text{diag}(e^r) \in \mathbb{R}_+^{q_i}$  for some free parameter vector  $r \in \mathbb{R}^{q_i}$ . The continuously differentiable and radially unbounded Hamiltonian function  $H_i : \mathbb{R}^{q_i} \rightarrow \mathbb{R}_+$  of  $\Sigma_{pH,i}$  represents the energy of  $i^{\text{th}}$  controller and is endowed with some parameters  $\vartheta_i$ . Moreover, we collect all the optimization parameters of  $i^{\text{th}}$  sub-controller in a set  $\theta_i := \{J_i, \Lambda_i, \vartheta_i, G_i\}$ . For the sake of presentation, the distributed controller (9) can be compactly written as

$$\Sigma_{pH} : \begin{cases} \dot{\xi}(t) = [J_c - (\alpha I + \Lambda)] \frac{\partial H_c}{\partial \xi}(\xi, \vartheta) + G_c \mathbf{y}(t) \\ \mathbf{u}(t) = G_c^\top \frac{\partial H_c}{\partial \xi}(\xi, \vartheta), \end{cases} \quad (10)$$

where  $\xi \in \Xi_1 \times \dots \times \Xi_N \subseteq \mathbb{R}^{n_c}$ ,  $\mathbf{u} \in \mathcal{U}_{c,i} \times \dots \times \mathcal{U}_{c,N} \subseteq \mathbb{R}^m$ ,  $\mathbf{y} \in \mathcal{Y}_{c,i} \times \dots \times \mathcal{Y}_{c,N} \subseteq \mathbb{R}^m$  are stacked vectors of controller states, outputs, and inputs, respectively. The block matrix  $J_c = \text{blkdiag}(J_i)$  is skew-symmetric, and  $(\alpha I + \Lambda)$ ,<sup>4</sup> where  $\Lambda = \text{blkdiag}(\Lambda_i)$  is diagonal by construction, and the input matrix  $G_c = \text{blkSparse}(\mathcal{P}_c)$  is full rank.<sup>5</sup> Moreover, the Hamiltonian function  $H_c : \mathbb{R}^{n_c} \rightarrow \mathbb{R}_+$  of  $\Sigma_{pH}$  is the algebraic sum of all  $N$  sub-controllers' energies  $H_i$ , i.e.  $H_c(\xi, \vartheta) = \sum_{i \in \mathcal{V}_s} H_i(\xi_i(t), \vartheta_i)$ . Finally, we gather all the optimization parameters of the distributed controller (10) in a set  $\theta := \{J, \Lambda, \vartheta, G_c\}$ .

*Remark 2 (Selection of Hamiltonian):* We impose minimal restrictions on the Hamiltonian functions  $H_i(\xi_i, \vartheta_i)$ , i.e., differentiability and radial unboundedness. This flexibility allows using diverse parametrizations including simple quadratic functions, and NNs (as in [46], [47] for representing  $H_i$ ). Several NNs satisfy the mild assumptions above, for example:

- Multi-Layered Perceptron (MLPs) with SmoothReLU( $\cdot$ ) activation functions  $\tilde{\sigma}(\cdot)$

$$\begin{aligned} H_i(\xi_i, \vartheta_i) &= z_L \\ z_1 &= \tilde{\sigma}_1(W_1 \xi_i + b_1) \\ z_\ell &= \tilde{\sigma}_\ell(W_\ell z_{\ell-1} + b_\ell), \quad \ell = 2, \dots, L, \end{aligned}$$

<sup>4</sup>Note that the parametrization  $\alpha I + \Lambda$  is redundant, as the same set of matrices can be obtained by using  $\Lambda$  only. However, it makes it easier to enforce specific dissipativity properties as shown later in Section III.

<sup>5</sup>Decentralized control is achieved by setting  $G_c = \text{blkdiag}(G_i)$  in (10), making each sub-controller independent of the state of other subsystems or sub-controllers.

where  $L \geq 1$  represents the depth of the NN, and the parameters are  $\vartheta_i := \{W_L, \dots, W_1, b_1, \dots, b_L\}$ .

- Input Convex NNs (ICNNs) [48]

$$H_i(\xi_i, \vartheta_i) := \hat{\sigma}(\varphi_L(\xi_i) - \varphi(0)) + \epsilon \xi_i^\top \xi_i, \quad (11)$$

with  $\varphi_L$  defined as

$$\begin{aligned} z_1 &= \hat{\sigma}_1(W_1 \xi_i + b_1) \\ z_\ell &= \hat{\sigma}_\ell(U_\ell z_{\ell-1} + W_\ell \xi_i + b_\ell), \quad \ell = 2, \dots, L \\ \varphi_L(\xi_i) &= z_L, \end{aligned}$$

where  $\hat{\sigma}(\cdot)$  is a convex, monotonically non-decreasing, non-negative activation function, such as SmoothReLU( $\cdot$ ),  $W_\ell$  are real-valued weights,  $U_\ell$  are positive weights,  $b_\ell$  are real-valued biases, and  $\epsilon > 0$  is a small positive constant. In this case, we define  $\vartheta_i := \{W_1, \dots, W_L, U_2, \dots, U_L, b_1, \dots, b_L\}$ .

- Residual-like Networks [49]

$$H_i(\xi_i, \vartheta_i) := W_o z_L(\xi_i) + \epsilon \xi_i^\top \xi_i, \quad (12)$$

with  $z_L$  defined as

$$\begin{aligned} z_1 &= \sigma_1(W_1 \xi_i + b_1) \\ z_\ell &= \sigma_\ell(W_\ell z_{\ell-1} + b_\ell), \quad \ell = 2, \dots, L, \end{aligned}$$

where  $\sigma(\cdot)$  is a differentiable positive activation function, such as sigmoid( $\cdot$ ), SmoothReLU( $\cdot$ ), and Softplus( $\cdot$ ),  $\epsilon > 0$  is a small positive constant, and  $\vartheta_i := \{W_o, W_1, \dots, W_L, b_1, \dots, b_L\}$ .

Since all the aforementioned activation functions are differentiable and non-negative, the Hamiltonian  $H_i$  will also be differentiable and positive definite. Moreover, the radial unboundedness of the Hamiltonian is ensured by the use of unbounded activation functions for MLPs and the inclusion of quadratic terms  $\epsilon \xi_i^\top \xi_i$  in ICNNs and ResNet-like NNs.

In the sequel, we consider NN parametrizations of  $H_i$  because of their expressivity. Importantly, our results hold irrespective of the specific NN choice.

#### B. Solving the OCP (7)-(8)

There are various optimization methods for solving the finite-horizon OCP (7)-(8), including Sequential Quadratic Programming (SQP) [50], the Alternating Direction Method of Multipliers (ADMM) [51], the Augmented Lagrangian Alternating Direction Inexact Newton (ALADIN) method [52], and nonlinear interior point methods such as IPOPT [53]. In this paper, we leverage the well-established BackPropagation-Through-Time (BPTT) approach [54], [55] to solve (7)-(8) by reducing it to a NN training problem, where the optimization parameters  $\theta$  are referred as trainable parameters. This approach offers several advantages, including improved scalability through GPU parallelization, the ability to parametrize highly nonlinear functions via NNs, the potential to deal with high dimensionality in both parameter and state space, and to cater longer time horizons [13]. We defer the reader to Appendix E for a brief summary of BPTT. However, we highlight that the unconstrained parametrization of controllers with a finite  $\mathcal{L}_2$  or  $i\mathcal{L}_2$  gain in the following sections is independent of the chosen optimization method.

### III. $\mathcal{L}_2$ -STABLE HAMILTONIAN CONTROLLERS

The following result presents a parametrization of the controller  $\Sigma_{pH}$  that guarantees a finite  $\mathcal{L}_2$  gain regardless of the choice of the parameters  $\theta$  in (10). The proof is provided in Appendix A.

*Theorem 3:* Given a constant  $\epsilon > 0$ ,  $H_c(\xi, \cdot) \geq 0$ , set  $\alpha = \epsilon \bar{\lambda}(\mathbf{G}_c \mathbf{G}_c^\top)$  in (10). Then, the controller  $\Sigma_{pH}$  is  $\epsilon$ -output strictly passive, and has a finite  $\mathcal{L}_2$ -gain  $\leq 1/\epsilon$ .

In simple words, Theorem 3 implies that for any choice of parameters  $\theta$ , one can always choose a sufficiently large damping  $\alpha$  such that the controller  $\Sigma_{pH}$  is  $\epsilon$ -output strictly passive, and consequently, the map from  $\mathbf{y}(t) \mapsto \mathbf{u}(t)$  has a finite  $\mathcal{L}_2$  gain. Therefore, one can leverage Theorems 1 and 3 to ensure closed-loop stability in cases where the system  $\Sigma_s$  is passive or has a finite  $\mathcal{L}_2$  gain. While  $\alpha$  depends on the free parameters  $\mathbf{G}_c$ , we highlight that the parametrization in Theorem 3 is still unconstrained since it verifies the property (5) by design. Remark 8 in Appendix E outlines a brief procedure for the computation of  $\alpha$ , when using BPTT for optimizing the cost.

*Remark 3 (Comparison with RENs):* RENs [11] provide another class of models that can provide a finite  $\mathcal{L}_2$  gain and are parametrized in an unconstrained way. However, differently from RENs, our parametrization allows for incorporating diverse sparsity patterns within the weight matrices. Moreover, our method overcomes the limitation of RENs to use only quadratic storage functions. A precise comparison with the modeling capabilities of RENs is difficult. Nevertheless, Theorem 3 offers an alternative way to parametrize  $\mathcal{L}_2$  operators.

*Remark 4 (Learning models with finite  $\mathcal{L}_2$  gains):* Basically, the model (10) can be also interpreted as a Neural Ordinary Differential Equation (NODE) – a family of continuous-depth NNs represented by dynamical systems – [55] with a given distributed structure and built-in  $\mathcal{L}_2$  stability properties. Thus, besides control, it can be used for the identification of nonlinear interconnected systems that are known to be  $\mathcal{L}_2$  stable *a priori*. While the only limitation is that the number of inputs and outputs must coincide, the possibility of embedding the  $\mathcal{L}_2$  stability and the interconnection structure of the distributed system in the identification process is expected to improve the identification results.

### IV. INCREMENTALLY $\mathcal{L}_2$ -STABLE HAMILTONIAN CONTROLLERS

In the previous section, we demonstrated how to guarantee a finite  $\mathcal{L}_2$  gain of the pH controller (10). In this section, we provide formal guarantees for a finite  $i\mathcal{L}_2$  gain. Following the Definition 3, one can write the variational dynamics for the controller  $\Sigma_{pH}$  as

$$\begin{aligned} \delta \dot{\xi}(t) &= (\mathbf{J}_c - (\alpha \mathbf{I} + \mathbf{\Lambda})) \frac{\partial^2 H_c(\xi, \vartheta)}{\partial \xi^2} \delta \xi + \mathbf{G}_c \delta \mathbf{y}(t) \\ \delta \mathbf{u}(t) &= \mathbf{G}_c^\top \frac{\partial^2 H_c(\xi, \vartheta)}{\partial \xi^2} \delta \xi. \end{aligned} \quad (13)$$

Moreover, for (13), differential dissipativity models the “energy” dissipation of variations of the system trajectory. If the energy of these variations in the system trajectories

decreases over time, the trajectory variation will eventually only be determined by the system input. In order to define an incremental  $\mathcal{L}_2$  gain, one can choose the supply rate as  $s_\delta(\delta \mathbf{u}(t), \delta \mathbf{y}(t)) = \frac{1}{2} \gamma_\delta^2 \|\delta \mathbf{y}(t)\| - \frac{1}{2} \|\delta \mathbf{u}(t)\|$ ,  $\gamma_\delta > 0$  [22].

The following result, whose proof is given in Appendix B provides an unconstrained parametrization of pH controllers  $\Sigma_{pH}$  that enjoy a finite  $i\mathcal{L}_2$  gain.

*Theorem 4:* Given a constant  $\epsilon > 0$ , define  $\alpha = \epsilon_\delta \bar{\lambda}(\mathbf{G}_c \mathbf{G}_c^\top)$ . Moreover, let  $H_c(\xi, \vartheta)$  be at least twice differentiable with respect to its first argument and its Hessian satisfy

$$0 < c_1 \mathbf{I} \leq \frac{\partial^2 H_c(\xi, \vartheta)}{\partial \xi^2} \leq c_2 \mathbf{I}, \quad (14)$$

where  $c_1$  and  $c_2$  are positive constants. Then, the controller  $\Sigma_{pH}$  is  $\epsilon_\delta$ -output strictly incremental passive and has a finite  $i\mathcal{L}_2$ -gain  $\leq 1/\epsilon_\delta$ .

Notably, the condition (14) on the Hessian of  $H_c(\cdot, \cdot)$  restricts the choice to strictly convex Hamiltonian functions. One choice is to use quadratic functions to parametrize  $H_c(\xi, \vartheta) = \xi^\top (\mathbf{X}^\top \mathbf{X} + \epsilon \mathbf{I}) \xi$ , where  $\mathbf{X} \in \mathbb{R}^{n_c \times n_c}$  is a matrix of optimization parameters and  $\epsilon > 0$  is a small positive constant. However, for some complex applications, the expressivity of quadratic Hamiltonian functions may be insufficient. In this paper, next, we provide several NN-based parametrizations that satisfy (14) by design.

*Remark 5 (Monotone networks):* The condition (14) can be satisfied by parametrizing the gradient of the Hamiltonians  $H_i(\xi_i, \vartheta_i)$  as

$$\frac{\partial H(\xi_i, \vartheta_i)}{\partial \xi_i} = z_1(\xi_i) + \epsilon \xi_i, \quad (15)$$

where  $z_1(\xi) = W_0^\top \sigma_m(W_0 \xi + b_0)$  is a single-layered NN that is monotone<sup>6</sup> with respect to  $\xi$  for all  $W_0 \in \mathbb{R}^{n_c \times n_c}$ ,  $\sigma_m(\cdot)$  is a monotonically increasing activation function whose derivative  $\sigma'_m(\cdot)$  satisfies  $0 \leq \sigma'_m(\cdot) \leq \bar{S}$ , and  $\epsilon > 0$  is a small positive constant. Recall that a function is convex if and only if the gradient of the function is monotone [56, Proposition B.9] and in view of (15), the Hamiltonian function  $H_i(\xi_i, \vartheta_i) = \int (z_1(\xi_i) + \epsilon \xi_i) d\xi_i$  is convex. Moreover, the Hessian of  $H_i(\xi_i, \vartheta_i)$  can be computed as

$$\frac{\partial^2 H_i(\xi_i, \vartheta_i)}{\partial \xi_i^2} = W_0^\top D(\cdot) W_0 + \epsilon \mathbf{I}_{q_i}.$$

Since the diagonal matrices  $D(\cdot) := \text{diag}(\sigma'(W_0(\cdot) + b_0))$  and verify  $0 \leq D(\cdot) \leq \bar{S}$ , the constants  $c_1$  and  $c_2$  in (14) can be easily computed as

$$c_1 = \epsilon, \quad c_2 = \bar{S} \bar{\lambda}(W_0^\top W_0) + \epsilon.$$

Note that the assumption that activation functions  $\sigma(\cdot)$  are monotonic is satisfied by almost every nonlinear activation function used in practice, e.g.,  $\tanh(\cdot)$ ,  $\text{SmoothReLU}(\cdot)$ ,  $\text{SmoothLeakyReLU}(\cdot)$ , and  $\text{sigmoid}(\cdot)$ .

*Remark 6 (ICNNs):* In Theorem 4 one can parametrize the Hamiltonian functions  $H_i(\xi_i, \vartheta_i)$  by ICNNs [48] given in

<sup>6</sup>In functional analysis, on a topological vector space  $\Xi$ , a non-linear operator  $z_1 : \Xi \rightarrow \Xi$  is said to be a monotone operator if  $\langle z_1(\xi_1) - z_1(\xi_2), \xi_1 - \xi_2 \rangle \geq 0$ .

Remark 2. Since (12) is strictly convex in  $\xi_i$ , the Hessian can be bounded by the constants  $c_1 I_{q_i}$  and  $c_2 I_{q_i}$ . These constants can be calculated using the *autograd* library of Pytorch [57], for example.

Furthermore, the strict convexity of  $H_c(\xi, \vartheta) = \sum_{i \in \mathcal{V}_s} H_i(\xi_i, \vartheta_i)$  follows from the fact that the sum of strictly convex functions is also strictly convex.

## V. DISSIPATION-PRESERVING DISCRETIZATION SCHEMES

Given a continuous-time passive system, its discretized counterpart may not enjoy the same properties, as highlighted in [58], and [59]. For instance, traditional discretization methods, such as zero-order hold, do not preserve passivity.<sup>7</sup> Several researchers have focused on geometric discretization schemes based on variational integration theory, including (Semi-) Implicit Euler, leap-frog, and Verlet integration methods [61]. While they can conserve structural properties such as *symplecticity*, and long-term energy stability, they do not preserve the passivity, finite  $\mathcal{L}_2$ , and  $i\mathcal{L}_2$  gains. Furthermore, discretized systems stemming from these methods may become unstable for a large sampling period as shown in [59] and also illustrated in Appendix D. In this section, we leverage state-of-the-art discrete gradient methods [38] to preserve the dissipative properties of pH controllers (10) after discretization. To this end, we define discretizations of the gradient  $\nabla H_c(\xi) \equiv \frac{\partial H_c(\xi)}{\partial \xi}$  to define a class of numerical integrators that exactly preserve the first integral  $H_c(\cdot)$ .

*Definition 4* ([62]): Let  $H : \mathbb{R}^n \mapsto \mathbb{R}$  be a differentiable function. Then  $\bar{\nabla}H : \mathbb{R}^{2n} \mapsto \mathbb{R}^n$  is a discrete gradient of  $H$  if it is continuous and satisfies

$$\begin{aligned} \bar{\nabla}H(\mathbf{x}, \tilde{\mathbf{x}})^\top (\tilde{\mathbf{x}} - \mathbf{x}) &= H(\tilde{\mathbf{x}}) - H(\mathbf{x}), \forall \mathbf{x}, \tilde{\mathbf{x}} \in \mathbb{R}^n, \\ \bar{\nabla}H(\mathbf{x}, \mathbf{x}) &= \nabla H(\mathbf{x}), \forall \mathbf{x} \in \mathbb{R}^n. \end{aligned}$$

Some well-known examples of discrete gradients are:

- the mean value (or averaged) discrete gradient [63]

$$\bar{\nabla}H(\mathbf{x}, \tilde{\mathbf{x}}) := \int_0^1 \nabla H((1-s)\mathbf{x} + s\tilde{\mathbf{x}}) ds;$$

- the midpoint (or Gonzalez) discrete gradient [62]

$$\begin{aligned} \bar{\nabla}H(\mathbf{x}, \tilde{\mathbf{x}}) &:= \nabla H\left(\frac{1}{2}(\mathbf{x} + \tilde{\mathbf{x}})\right) \\ &+ \frac{H(\tilde{\mathbf{x}}) - H(\mathbf{x}) - \nabla H\left(\frac{1}{2}(\mathbf{x} + \tilde{\mathbf{x}})\right)^\top (\tilde{\mathbf{x}} - \mathbf{x})}{|\tilde{\mathbf{x}} - \mathbf{x}|^2} (\tilde{\mathbf{x}} - \mathbf{x}) \end{aligned}$$

for  $\tilde{\mathbf{x}} \neq \mathbf{x}$ ;

- the coordinate increment discrete gradient (Itoh-Abe) [64] with each component given by

$$\begin{aligned} \bar{\nabla}H(\mathbf{x}, \tilde{\mathbf{x}})_i &:= \frac{H(\tilde{\mathbf{x}}_1, \dots, \tilde{\mathbf{x}}_i, \mathbf{x}_{i+1}, \dots, \mathbf{x}_n)}{\tilde{\mathbf{x}}_i - \mathbf{x}_i} \\ &- \frac{H(\tilde{\mathbf{x}}_1, \dots, \tilde{\mathbf{x}}_{i-1}, \mathbf{x}_i, \dots, \mathbf{x}_n)}{\tilde{\mathbf{x}}_i - \mathbf{x}_i} \end{aligned}$$

for  $1 \leq i \leq n$  and  $\tilde{\mathbf{x}}_i \neq \mathbf{x}_i$ .

For more details on these methods, see [38].

<sup>7</sup>We defer the reader to [60] for the formal definitions of the discrete-time notion of passivity.

Consider the following numerical discretization of controller (10)

$$\Sigma_{dpH} : \begin{cases} \frac{\xi_{k+1} - \xi_k}{h_\Delta} = (\mathbf{J}_c - (\alpha \mathbf{I} + \mathbf{\Lambda})) \bar{\nabla}H_c(\xi_{k+1}, \xi_k) \\ \quad + \mathbf{G}_c \mathbf{y}_k \\ \mathbf{u}_k = \mathbf{G}_c^\top \bar{\nabla}H_c(\xi_{k+1}, \xi_k), \end{cases} \quad (16)$$

where  $h_\Delta > 0$  is the sampling time, and  $\xi_k, \mathbf{y}_k, \mathbf{u}_k$  corresponds to  $\xi(kh_\Delta), \mathbf{y}(kh_\Delta)$ , and  $\mathbf{u}(kh_\Delta)$ , respectively. Let us choose  $\alpha = \epsilon \bar{\lambda}(\mathbf{G}_c \mathbf{G}_c^\top)$  as in Theorem 3 so that the continuous-time counterpart (10) has a finite  $\mathcal{L}_2$  gain. Our goal is to prove that for this choice of dissipation constant  $\alpha$ , the controller (16) preserves the  $\mathcal{L}_2$  gain. To this aim, the following result, whose proof is provided in Appendix C shows that the discrete-time controller is also  $\epsilon$ -output strictly passive.

*Theorem 5:*

Given a constant  $\epsilon > 0$ , let  $\alpha = \epsilon \bar{\lambda}(\mathbf{G}_c \mathbf{G}_c^\top)$ , and  $H_c(\xi, \cdot) \geq 0$ . Then, the discrete-time controller  $\Sigma_{dpH}$  is  $\epsilon$ -output strictly passive, and has a finite  $\mathcal{L}_2$ -gain  $\leq 1/\epsilon$ .

Unfortunately, the discrete-time dynamics (16) is implicit, that is,  $\xi_{k+1}$  appear on both sides of the dynamics, and the output equation  $\mathbf{u}_k = \mathbf{G}_c^\top \bar{\nabla}H_c(\xi_{k+1}, \xi_k)$  is non-causal. Note that having implicit forms in the dissipation-preserving discretization of pH systems is quite common [65]. Moreover, if  $H_c(\cdot, \cdot)$  is parametrized via a NN, the discrete-time dynamics (16) defines the forward equation of a well-known class of NNs called *implicit NNs*-see [11], [66]–[69], for example. The main challenge of employing implicit NNs in practice is to guarantee the existence and uniqueness of the solution of the forward equation. In our case, this amounts to show that the following implicit equation has a unique solution  $\xi_{k+1} \in \Xi$  for all  $\xi_k \in \Xi$  and  $\mathbf{y}_k \in \mathcal{Y}_c$

$$\begin{aligned} \xi_{k+1} &= \xi_k + h_\Delta (\mathbf{J}_c - (\alpha \mathbf{I} + \mathbf{\Lambda})) \bar{\nabla}H_c(\xi_{k+1}, \xi_k) \\ &+ h_\Delta \mathbf{G}_c \mathbf{y}_k. \end{aligned} \quad (17)$$

Sometimes, such implicit expressions can be easily solved for  $\xi_{k+1}$ , e.g. in the linear case [70]. Nevertheless, a sufficient condition on the existence and uniqueness of the solution of (17) is provided in [65]. This condition is based on the uniform boundness of  $\nabla H_c(\xi)$ , and the choice of discrete gradient used. The technical details have been omitted here.

*Remark 7* (Finite  $i\mathcal{L}_2$  gain): By selecting the dissipation  $\alpha \geq \epsilon_\delta \bar{\lambda}(\mathbf{G}_c \mathbf{G}_c^\top)$  in the pH controller (10) and the Hamiltonian function  $H_c$  such that it satisfies condition (14), the implicit discrete-time controller (16) has a finite  $i\mathcal{L}_2$  gain. This can be proved similarly as for Theorem 5.

## VI. EXPERIMENTS

In this section, we showcase the application of the proposed pH-based control framework via experiments. Specifically, we consider consensus control of non-holonomic wheeled robots, and power sharing and weighted voltage regulation in a DC microgrid. The readers are also referred to [39] for an additional example about the synchronization of Kuramoto oscillators using the pH controllers (10) endowed with a finite  $\mathcal{L}_2$  gain.

### A. Consensus of non-holonomic wheeled robots

We illustrate the efficacy of the pH controller (10) by considering a consensus problem with collision avoidance for a swarm of  $N$  non-holonomic physically decoupled agents such as wheeled mobile robots modeled as [71], [72]:

$$\begin{aligned}\dot{x}_i(t) &= (J_s(x_i) - R_s) \frac{\partial H(x_i)}{\partial x_i} + G(x_i) u_i(t) \\ y_i(t) &= G(x_i)^\top \frac{\partial H(x_i)}{\partial x_i},\end{aligned}\quad (18)$$

where  $x_i = [q_i^\top, p_i^\top]^\top \in \mathbb{R}^n$ , and  $q_i = [q_{x,i}, q_{y,i}, q_{\theta,i}]$  are generalized coordinates and  $p_i = [p_{v,i}, p_{\omega,i}]$  are transformed generalized momenta for  $i^{\text{th}}$  robot as depicted in Fig. 3. Moreover, the matrix-valued functions in (18) are given as:

$$\begin{aligned}J_s(x_i) &= \begin{bmatrix} 0_{3 \times 3} & S(x_i) \\ -S^\top(x_i) & C(x_i) \end{bmatrix}, \\ S(x_i) &= \begin{bmatrix} \cos q_{\theta,i} & -d \sin q_{\theta,i} \\ \sin q_{\theta,i} & d \cos q_{\theta,i} \\ 0 & 1 \end{bmatrix}, \\ C(x_i) &= \begin{bmatrix} 0 & \frac{md}{md^2 + \Omega_m} p_{\omega,i} \\ -\frac{md}{md^2 + \Omega_m} p_{\omega,i} & 0 \end{bmatrix}, \\ R_s &= 0.05I_5, \quad G(x_i) = \begin{bmatrix} 0_{3 \times 2} \\ I_2 \end{bmatrix}.\end{aligned}\quad (19)$$

In (18),  $H_i(x_i) = \frac{1}{2} p^\top M p$ ,  $M = \text{blkdiag}(m, \Omega_m + md^2)$  is the kinetic energy of an individual robot, where  $m = 6.0Kg$ ,  $\Omega_m = 0.1Kgm^2$ , and  $d = 0.2m$ . For further details about model (18), we defer the reader to [71], and [72].

Our goal is to minimize the following loss function:

$$\int_0^T (\ell_1(\mathbf{x}(t)) + \ell_2(\mathbf{x}(t))) dt \quad (20)$$

with the consensus-promoting term

$$\ell_1(\mathbf{x}(t)) = \frac{1}{N^2} \sum_{i=1}^N \sum_{j=1}^N \|v_i - v_j\|,$$

and the collision-avoidance term

$$\ell_2(\mathbf{x}(t)) = \begin{cases} \frac{1}{N^2} \sum_{i=1}^{N-1} \sum_{j=i+1}^N \frac{1}{(r_{ij} + \epsilon)^2}, & \text{if } r_{ij} < \bar{r} \\ 0 & \text{otherwise,} \end{cases}$$

where  $v_i$  is the forward velocity of agent  $i$ ,  $r_{ij}$  is the relative distance between an agent  $j$  and an agent  $i$ ,  $\bar{r} > 0$  is a constant that defines the collision-avoidance distance, and  $\epsilon > 0$  is a small positive constant for numerical stability. Since the radius of each robot is  $0.2m$ , a relative distance of  $r_{ij} < 0.5m$  (from the center of the  $i^{\text{th}}$  robot to the center of the  $j^{\text{th}}$  robot) will denote a collision, therefore, in this experiment, we set  $\bar{r} = 0.8m$ . To compute the loss function (20), the relative distance  $r_{ij}$  can be calculated as  $r_{ij} = \sqrt{(q_{x,i} - q_{x,j})^2 + (q_{y,i} - q_{y,j})^2}$  and  $v_i$  in  $\ell_1(\mathbf{x}(t))$  is computed as  $p_{v,i}/m$ ,  $\forall i \in \mathcal{V}_s$ .

It is well known that dynamical systems subject to non-holonomic constraints violate *Brockett's necessary condition* for asymptotic stabilizability, meaning they cannot be stabilized using a continuous state-feedback policy [22, Section 6.4]. This motivates the use of time-varying and discontinuous controllers, such as those parametrized by pH controllers (10)

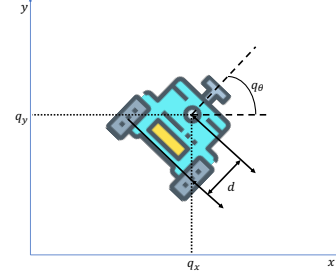


Fig. 3: The mobile wheeled robot used in the experiment. The triple  $(q_x, q_y, q_\theta)$  denotes the position and the orientation of the robot, and  $d$  is the distance from the center to the wheels.

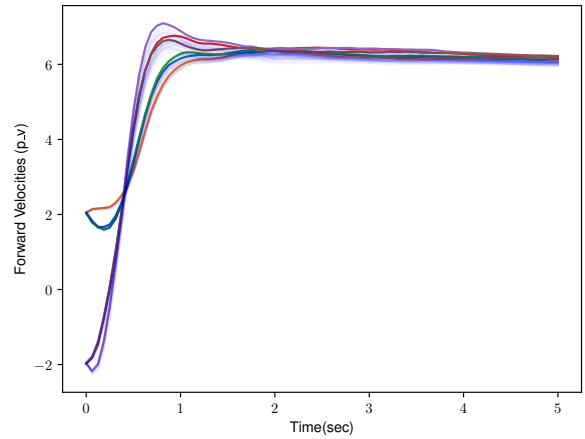


Fig. 4: Forward velocities of the swarm demonstrating consensus. The translucent blue color lines represent the evolution of trajectories starting from the initial conditions sampled from a ball with radius 0.05 centered at the nominal condition for each agent.

with time-varying parameters for  $t \leq T$ , while minimizing the nonlinear objective function (20). For  $t > T$ , we freeze the parameters of the controller, as discussed in Remark 1.

To solve the OCP with loss function (20), we trained the distributed pH controller (10), where we set  $J_c = \text{blkdiag}(J_i)$ , with  $J_i = I_2 \otimes \begin{bmatrix} 0 & 1 \\ -1 & 0 \end{bmatrix}$ ,<sup>8</sup>  $\alpha = 0.125\bar{\lambda}(\mathbf{G}_c \mathbf{G}_c^\top)$  as in Theorem 3,  $\mathbf{\Lambda} \equiv 0$ , and  $\mathbf{G}_c = \text{blkSparse}(\mathcal{P})$ , where  $\mathcal{P} \in \mathbb{R}^{N \times N}$  is the adjacency matrix. To have more flexibility during the finite horizon  $T$ , we choose a time-varying Hamiltonian function for  $i$ -th controller, i.e.  $H_c(\xi_i, t) = \log[\cosh(K_i(t)\xi_i + b_i(t))]^\top \mathbf{1}$  for  $t \in [0, T]$ , where  $K_i : \mathbb{R} \rightarrow \mathbb{R}^{4 \times 4}$  and  $b_i : \mathbb{R} \rightarrow \mathbb{R}^4$  are piecewise constant optimization parameters. In this investigation, we consider  $N = 6$  agents communicating over a network with an undirected cyclic graph topology, i.e. whose

<sup>8</sup>Here,  $\otimes$  denotes the standard Kronecker product.



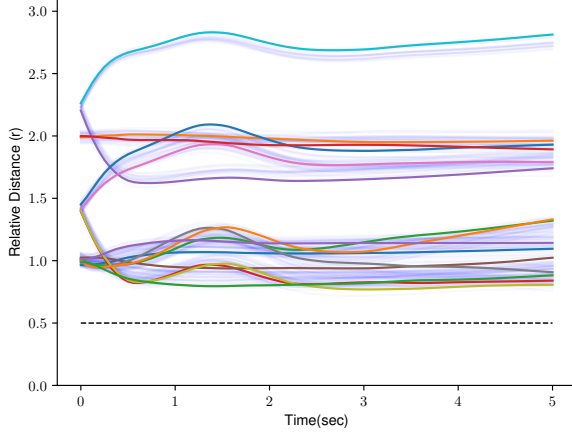


Fig. 5: Relative distance  $r_{ij}$  among the agents with collision avoidance. Note that  $r_{ij} < 0.5$  indicates a collision. The translucent blue color lines represent the evolution of trajectories starting from the initial conditions sampled from a ball with radius 0.05 centered at the nominal condition for each agent.

adjacency matrix is given by

$$\mathcal{P} = \begin{bmatrix} 2 & -1 & 0 & 0 & 0 & -1 \\ -1 & 2 & -1 & 0 & 0 & 0 \\ 0 & -1 & 2 & -1 & 0 & 0 \\ 0 & 0 & -1 & 2 & -1 & 0 \\ 0 & 0 & 0 & -1 & 2 & -1 \\ -1 & 0 & 0 & 0 & -1 & 2 \end{bmatrix}.$$

Then, we optimize the parameters  $\theta = \{\mathbf{K}, \mathbf{b}, \mathbf{G}_c\}$  using BPTT in PyTorch [57]. Particularly, we choose  $S = 20$  initial conditions sampled uniformly in a ball of radius 0.05 centered at nominal initial condition  $\mathbf{x}_0$  for each agent. The whole training procedure takes almost 10 mins on a Bizon ZX5000 G2 workstation. For more details, we defer the reader to Appendix E.

After optimization, we simulate the closed-loop system. Fig. 4 demonstrates the consensus among all agents in terms of forward velocities, while Fig. 5 displays the relative distances among the agents initialized from various initial conditions. Since the relative distances  $r_{ij} > 0.5, \forall i, j \in \mathcal{V}_s$ , the pH controller has effectively achieved collision avoidance. Moreover, in both figures, the translucent blue trajectories demonstrate that the pH controller managed to achieve the goals for new test points sampled near the nominal initial conditions, indicating a degree of robustness to out-of-sample distributions.

### B. Power sharing and averaged voltage regulation in DC microgrids

In this experiment, we explore weighted power sharing and averaged voltage regulation in DC microgrids. The model of a DC microgrid consists of  $N$  Distributed Generation Units (DGUs) connected by  $M$  resistive-inductive (RL) power lines

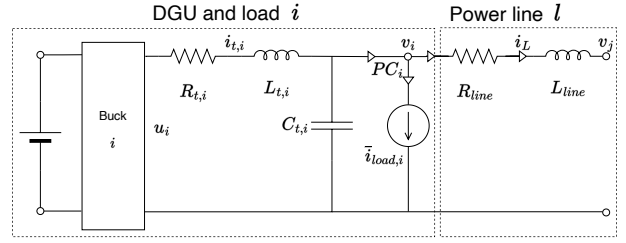


Fig. 6: The electric scheme of  $i^{th}$  DGU and the collocated load.

[73]. An electrical circuit diagram of a typical DGU with its load is provided in Fig. 6. The overall DC microgrid can be described as follows [73]:

$$\Sigma_{dmG} := \begin{cases} \mathbf{C}_t \dot{\mathbf{v}} = \mathbf{i}_t + \mathbf{B} \mathbf{i}_L - \mathbf{i}_{load} \\ \mathbf{L}_t \dot{\mathbf{i}}_t = -\mathbf{v} - \mathbf{R}_t \mathbf{i}_t + \mathbf{u}(t) \\ \mathbf{L}_{line} \dot{\mathbf{i}}_L = -\mathbf{B} \mathbf{v} - \mathbf{R}_{line} \mathbf{i}_L \\ \mathbf{y}(t) = \mathbf{i}_t, \end{cases}$$

where  $\mathbf{i}_t$  and  $\mathbf{v} \in \mathbb{R}^N$  represent the stacked filter (generator) currents and the voltages at the points of connection, respectively, while  $\mathbf{i}_L \in \mathbb{R}^M$  denotes the vector of line currents. The control input  $\mathbf{u}(t)$  is the stacked vector of all the command signals to DC-DC Buck converters, and  $\mathbf{i}_{load}$  collects all the currents drawn by the loads collocated with DGUs. For the sake of this experiment, we assume that the electrical and communication interconnections are identical and are given by the graph in Fig. 7 whose incidence matrix is:

$$\mathbf{B} = \begin{bmatrix} 1 & 0 & 1 & 0 & 0 & 1 & 0 \\ -1 & 1 & 0 & 0 & 0 & 0 & 0 \\ 0 & 0 & -1 & 1 & 0 & 0 & 0 \\ 0 & -1 & 0 & -1 & 1 & 0 & 0 \\ 0 & 0 & 0 & 0 & -1 & 0 & -1 \\ 0 & 0 & 0 & 0 & 0 & -1 & 1 \end{bmatrix}. \quad (21)$$

The graph adjacency matrix is therefore defined as  $\mathcal{P}_e = \mathbf{B} \Gamma_w \mathbf{B}^T$ , where  $\Gamma_w$  are the weights of the edges. All the parameters of the DC microgrid considered in this experiment are given in Table I, while the interconnection of the DGUs and corresponding line parameters  $R_{ij}, L_{ij}$  are provided in Fig. 7. We consider loads modeled by an impedance and a constant current, i.e.  $\mathbf{i}_{load} = \mathbf{Y}_{load} \mathbf{v} + \bar{\mathbf{i}}_{load}$ . Additionally,  $\mathbf{C}_t$ ,  $\mathbf{L}_t$ ,  $\mathbf{Y}_{load}$ , and  $\mathbf{R}_t \in \mathbb{R}^{N \times N}$ , as well as  $\mathbf{R}_{line}$  and  $\mathbf{L}_{line} \in \mathbb{R}^{M \times M}$ , are positive definite diagonal matrices. For example,  $\mathbf{C}_t = \text{diag}(C_1, \dots, C_N)$ , where  $C_i$  represents the capacitance (combined with line capacitances) of the DC converters, and  $\mathbf{L}_t$  and  $\mathbf{R}_t$  represent the internal inductances and resistances. Finally,  $\mathbf{R}_{line}$  and  $\mathbf{L}_{line}$  correspond to the inductances and resistances of the power lines connecting the DGUs.

The objective of this experiment is to design a distributed control scheme that ensures fair power sharing among the DGUs in the DC microgrid  $\Sigma_{dmG}$  while regulating the weighted average voltage. This can be formulated as a control

# DGU	$R(\Omega)$	$C_t(mF)$	$L_t(mH)$	$Y_{load}(m\Omega^{-1})$	$\bar{i}_{load}(A)$
1	0.2	2.2	1.8	0.333	1.67
2	0.3	1.9	2.0	0.370	2.00
3	0.1	1.7	2.2	0.303	2.33
4	0.5	2.5	3.0	0.303	2.17
5	0.4	2.0	1.3	0.333	2.67
6	0.6	3.0	2.5	0.317	2.50

TABLE I: Electrical parameters for the DC microgrid.

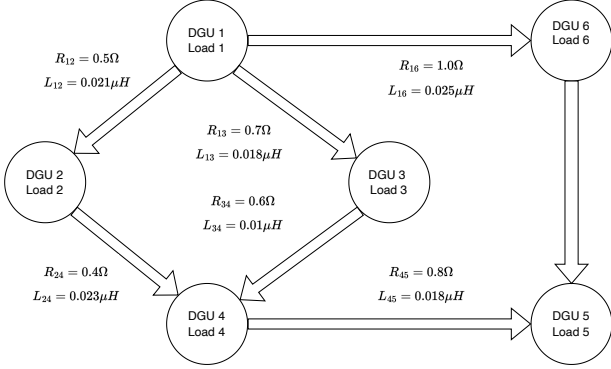


Fig. 7: Representation diagram of the DC microgrid with line parameters. The arrows show the reference system for positive currents. The undirected communication topology among DGUs' controllers is given by the same graph by ignoring the arrows.

objective to ensure that the following conditions are satisfied at the steady state:

$$w_i P_i = w_j P_j, \forall i, j \in \mathcal{V}_s, \quad (22)$$

where the power  $P_i$  flowing out of  $i^{th}$  DGU converges to its steady state solution for all  $i \in \mathcal{V}_s$ , i.e.,

$$\lim_{t \rightarrow \infty} P_i(t) = \bar{P}_i, \quad (23)$$

where  $\bar{P} = \bar{w} P^*$ ,  $P^* \in \mathbb{R}$  with  $\bar{w} = [1/w_1, \dots, 1/w_N]^T$ ,  $w_i > 0$  for all  $i \in \mathcal{V}_s$  and any scalar  $P^*$ , which is the sum of the powers drawn by each load. The value of  $P^*$  can be calculated using steady-state values of voltages and load currents, see [74, Chapter 5] for more details. For our experiment, the computed value is  $P^* = 671.57W$ . To regulate weighted average voltage, all DGUs in the network should converge to a preset reference value  $v^*$ . In this context, the DGU with the largest capacity is assigned the highest weight, leading to the following objective:

$$\lim_{t \rightarrow \infty} \sum_{i=1}^N \bar{w}_i v_i(t) = \sum_{i=1}^N \bar{w}_i v^*,$$

where  $v^* = 50V$ . Moreover, it is also desired that all the individual voltages of DGUs, i.e.  $v_i(t)$  should remain within  $\pm 5\%$  of  $v^*$  [75]. Finally, since the dynamics  $\Sigma_{mdG}$  are linear and incrementally stable [76], it is important to preserve the  $i\mathcal{L}_2$  gain of the closed-loop for good reference tracking. Accordingly, the OCP can be formulated as follows:

$$\min_{\theta} \frac{1}{S} \sum_{k=1}^S c(\mathbf{x}(t), \mathbf{u}(t); \theta, \mathbf{x}_0^k)$$

$$c(\mathbf{x}(t), \mathbf{u}(t), \mathbf{x}_0) = \frac{1}{2NT} \int_0^T \sum_{i=1}^N (\|\bar{w}_i v_i(s) - \bar{w}_i v^*\| + \|v_i(s) i_{t,i}(s) - \bar{w}_i P^*\|) ds,$$

such that  $\Sigma_{dmG} \|f \Sigma_{pH}$  has a finite  $i\mathcal{L}_2$  gain. For this OCP, we choose  $\bar{w} = [0.3, 0.1, 0.05, 0.15, 0.22, 0.18]^T$ .

Note that similar optimization problems have already been addressed in several works as reviewed in [77]. Our main goal is not to outperform state-of-the-art solutions but to demonstrate power sharing and voltage balancing by solving a single OCP via the pH controller (10). Moreover, our approach paves the way for the use of more complex control costs that, in addition to the above goals, can account for nonlinear phenomena, such as component aging or nonlinear loads.

In this experiment, for the pH controller (10), we set  $J_c = \text{blkdiag}(J_i)$  where  $J_i = \Gamma_i - \Gamma_i^T$  and  $\Gamma_i \in \mathbb{R}^{3 \times 3}$  are lower triangular matrices,  $\Lambda = 10I_{18}$ ,  $G_c = \text{blkSparse}(\mathcal{P}_e)$ ,  $\alpha = 2.0\lambda(G_c G_c^T)$  and the Hamiltonian function  $H_c(\xi) = \log(\cosh[\text{blkdiag}(K_i)\xi])^T \mathbf{1} + 0.1\xi^T \xi$ , with  $K_i \in \mathbb{R}^{3 \times 3}$ . We choose  $S = 1$  in this example. However, after training, we simulated the closed-loop on different initial conditions to validate the performance. The whole training procedure takes almost 1.5 hours on a Bizon ZX5000 G2 workstation. See Appendix E for more details on the training.

Once the training is done, we simulated the closed-loop  $\Sigma_{dmG} \|f \Sigma_{pH}$  and both the regulation of weighted voltage and the power-sharing are showcased in Figs. 8, and 9, respectively. The results indicate that the distributed pH controller has successfully achieved the desired reference voltage  $v^*$  and averaged power  $P^*$ , which represents the total load requirement of the entire microgrid. Moreover, in Fig. 10, we present trajectories of averaged voltages of DGUs for 10 randomly chosen initial conditions converging to  $v^*$  demonstrating good reference tracking. Finally, Fig. 11 displays the individual voltages at the points of connection of each DGU remaining within the normal operating range of  $\pm 5\%$  around  $v^*$ , hence, demonstrating the efficacy of the proposed pH-based control framework.

## VII. CONCLUSION AND OUTLOOK

The distributed control of large-scale nonlinear systems can pose several challenges, such as guaranteeing closed-loop stability. To tackle this issue, we have proposed an unconstrained parametrization of distributed controllers via Hamiltonian models that preserve closed-loop stability and guarantee a finite  $\mathcal{L}_2$  or an  $i\mathcal{L}_2$  gain, for arbitrarily large networks of nonlinear dissipative systems. We provided discretization schemes that can preserve these dissipative properties for implementation purposes. We demonstrated that near-optimal performance can be achieved by parametrizing nonlinear storage functions via some NNs for the controllers. Moreover, these NN structures can be leveraged for nonlinear system

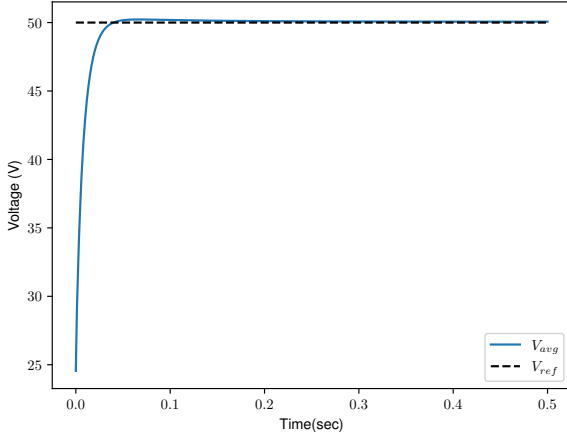


Fig. 8: Averaged voltage of the whole microgrid.

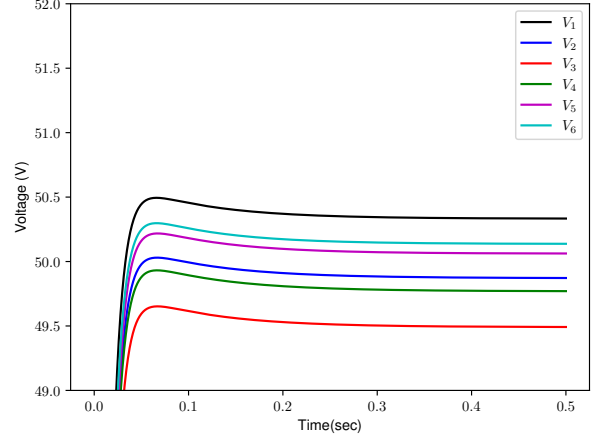


Fig. 11: Voltages of individual DGUs.

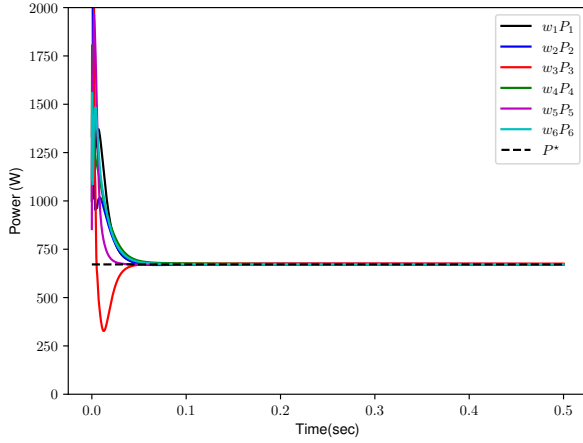


Fig. 9: Weighted averaged power converging to  $P^*$ .

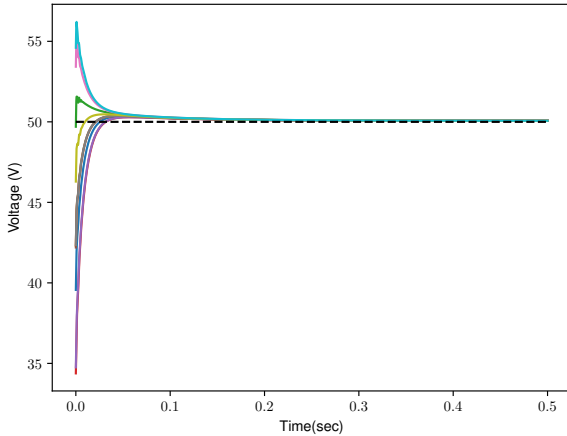


Fig. 10: Averaged voltage of the whole microgrid for 10 random initial conditions.

identification from data, where for example, the identified models are stable by design and have a finite  $\mathcal{L}_2$  gain.

Further efforts will be devoted to implementing the controllers on real-world systems and also to generalize the framework beyond pH models.

## APPENDIX

### A. Proof of Theorem 3

The proof is done by showing that the controller (10) is  $\epsilon$ -strictly output passive for  $\alpha \geq \epsilon \bar{\lambda}(\mathbf{G}_c \mathbf{G}_c^\top)$ . Recall from [22], that the controller (10) is  $\epsilon$ -output strictly passive if and only if the following conditions hold  $\forall \xi \in \Xi$

$$\frac{\partial}{\partial \xi} V f(\xi) \leq -\epsilon h^\top(\xi) h(\xi) \quad (24a)$$

$$\frac{\partial}{\partial \xi} V g(\xi) = h^\top(\xi), \quad (24b)$$

where  $V(\xi)$  is a  $C^1$  storage function and satisfies  $V \geq 0$ .

Moreover,  $f(\xi) = (\mathbf{J}_c - (\alpha \mathbf{I} + \mathbf{\Lambda})) \frac{\partial H(\xi, \vartheta)}{\partial \xi}$ ,  $g(\xi) = \mathbf{G}_c$ , and  $h(\xi) = \mathbf{G}_c^\top \frac{\partial H(\xi, \vartheta)}{\partial \xi}$ . First, we show that inequality 24a is satisfied by design. Let us choose the candidate storage function as the Hamiltonian of controller (10), i.e.  $V(\xi) = H_c(\xi, \vartheta) \geq 0$ , then we have

$$\begin{aligned} \frac{\partial^\top H(\xi)}{\partial \xi} f(\xi) &\leq -\epsilon h^\top(\xi) h(\xi), \quad \forall \xi \in \Xi \\ \frac{\partial^\top H(\xi)}{\partial \xi} (\mathbf{J} - (\alpha \mathbf{I} + \mathbf{\Lambda})) \frac{\partial H(\xi)}{\partial \xi} &\leq -\epsilon \frac{\partial^\top H(\xi)}{\partial \xi} \mathbf{G}_c \mathbf{G}_c^\top \frac{\partial H(\xi)}{\partial \xi} \\ \frac{\partial^\top H(\xi)}{\partial \xi} \left( -\alpha \mathbf{I} - \mathbf{\Lambda} + \epsilon \mathbf{G}_c \mathbf{G}_c^\top \right) \frac{\partial H(\xi)}{\partial \xi} &\leq 0. \end{aligned}$$

Therefore, choosing  $\alpha \geq \epsilon \bar{\lambda}(\mathbf{G}_c \mathbf{G}_c^\top)$  verifies the last inequality. Note that the second equality (24b) is verified by construction due to the choice of storage function and the structure of the pH controller (10). Finally, by employing [22, Theorem 2.2.13] we conclude that if the controller (10) is  $\epsilon$ -output strictly passive, then it has a finite  $\mathcal{L}_2$ -gain  $\leq 1/\epsilon$  for all trainable parameters  $\theta$ .  $\square$

### B. Proof of Theorem 4

First, let us show that differential controller (13) is  $\epsilon_\delta$ -output strictly incrementally passive with a suitable storage function. To this aim, recall from [22], that the controller (10) is strictly output passive if and only if the following conditions hold  $\forall \xi$

$$\frac{\partial}{\partial \xi} V_\delta f(\xi, \delta \xi) \leq -\epsilon_\delta h^\top(\xi, \delta \xi) h(\xi, \delta \xi), \quad (25a)$$

$$\frac{\partial}{\partial \xi} V_\delta g(\xi, \delta \xi) = h^\top(\xi, \delta \xi), \quad (25b)$$

where  $V_\delta(\xi, \delta \xi)$  is a storage function for variational dynamics (13) and  $\epsilon_\delta > 0$  is a positive constant. Moreover,

$$f(\xi, \delta \xi) = (\mathbf{J} - (\alpha \mathbf{I} + \mathbf{\Lambda})) \frac{\partial^2 H_c(\xi, \vartheta)}{\partial \xi^2} \delta \xi, \quad g(\xi, \delta \xi) = \mathbf{G}_c$$

$$h(\xi, \delta \xi) = \mathbf{G}_c^\top \frac{\partial^2 H_c(\xi, \vartheta)}{\partial \xi^2} \delta \xi,$$

respectively. Consider the storage function  $V_\delta(\xi, \delta \xi) = \frac{1}{2} \delta \xi^\top \frac{\partial^2 H(\xi, \vartheta)}{\partial \xi^2} \delta \xi$ , that verifies  $V_\delta(\cdot, 0) = 0$ , and  $V_\delta(\cdot, \cdot) > 0$ . The latter inequality can be verified by the condition 14. Then, for the inequality (25a), we obtain

$$\begin{aligned} \delta \xi^\top \frac{\partial^2 H(\xi)}{\partial \xi^2} (\mathbf{J} - (\alpha \mathbf{I} + \mathbf{\Lambda})) \frac{\partial^2 H(\xi)}{\partial \xi^2} \delta \xi \leq \\ -\epsilon_\delta \delta \xi^\top \frac{\partial^2 H(\xi)}{\partial \xi^2} \mathbf{G}_c \mathbf{G}_c^\top \frac{\partial^2 H(\xi)}{\partial \xi^2} \delta \xi. \end{aligned}$$

Thus, by choosing  $\alpha \geq \epsilon_\delta \bar{\lambda}(\mathbf{G}_c \mathbf{G}_c^\top)$ , the differential controller is  $\epsilon_\delta$ -output strictly incrementally passive and the finite  $i\mathcal{L}_2$  gain is less than  $1/\epsilon_\delta$  [22, Proposition 2.2.21]. Finally, the incremental dissipativity of the controller (10) with  $\alpha \geq \epsilon_\delta \bar{\lambda}(\mathbf{G}_c \mathbf{G}_c^\top)$  follows from [45, Theorem 6].  $\square$

### C. Proof of Theorem 5

Our goal is to show that

$$\frac{H_c(\xi_{k+1}) - H_c(\xi_k)}{h_\Delta} \leq s(\mathbf{u}_k, \mathbf{y}_k) \quad (26)$$

where  $s(\mathbf{u}_k, \mathbf{y}_k)$  is a supply-rate, and  $h_\Delta > 0$  is an arbitrary step-size. Let us consider the following supply rate [78]

$$s(\mathbf{u}_k, \mathbf{y}_k) = \mathbf{u}_k^\top \mathbf{y}_k - \epsilon \|\mathbf{u}_k\|_2^2.$$

Then, by using the definition of discrete gradient (Definition 4), we obtain

$$\begin{aligned} H_c(\xi_{k+1}) - H_c(\xi_k) &= \bar{\nabla} H_c(\xi_k, \xi_{k+1})^\top (\xi_{k+1} - \xi_k) \\ &= \bar{\nabla} H_c^\top (h_\Delta (\mathbf{J}_c - (\alpha \mathbf{I} + \mathbf{\Lambda})) \bar{\nabla} H_c + h_\Delta \mathbf{G}_c \mathbf{y}_k) \\ &= \bar{\nabla} H_c^\top (-h_\Delta (\alpha \mathbf{I} + \mathbf{\Lambda}) \bar{\nabla} H_c + h_\Delta \mathbf{G}_c \mathbf{y}_k) \\ &\leq h_\Delta \mathbf{u}_k^\top \mathbf{y}_k - h_\Delta \epsilon \|\mathbf{u}_k\|_2^2. \end{aligned}$$

By setting  $\mathbf{u}_k = \mathbf{G}_c^\top \bar{\nabla} H_c$ , we can cancel  $h_\Delta \bar{\nabla} H_c^\top \mathbf{G}_c \mathbf{y}_k$  on both sides and then, after dividing the inequality by  $h_\Delta > 0$ , we get

$$\bar{\nabla} H_c^\top (-(\alpha \mathbf{I} + \mathbf{\Lambda}) \bar{\nabla} H_c + \mathbf{G}_c \mathbf{y}_k) \leq \mathbf{u}_k^\top \mathbf{y}_k - \epsilon \|\mathbf{u}_k\|_2^2.$$

Therefore, by choosing  $\alpha \geq \epsilon \bar{\lambda}(\mathbf{G}_c \mathbf{G}_c^\top)$  and discretizing through a discrete gradient method, one can preserve the finite  $\mathcal{L}_2$  gain.  $\square$

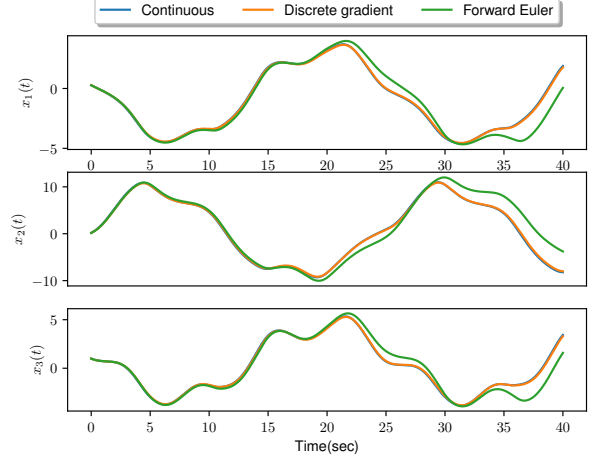


Fig. 12: Evolution of trajectories for a random initial condition.

### D. Dissipation-preserving discretization of pH controllers

In this investigation, we demonstrate discretization using discrete-gradient methods, such as the Itoh-Abe method [38], preserves the  $\mathcal{L}_2$  gain, while some common discretization schemes such as Forward Euler do not.

Consider the continuous-time pH controller  $\Sigma_{pH}$  (10) with parameters

$$\mathbf{J}_c = \begin{bmatrix} 0 & -1 & 0 \\ 1 & 0 & 1 \\ 0 & -1 & 0 \end{bmatrix}, \quad \mathbf{G}_c = \begin{bmatrix} 0.5 \\ 1.0 \\ 1.0 \end{bmatrix}.$$

Moreover, set  $\alpha = 0.001 \bar{\lambda}(\mathbf{G}_c \mathbf{G}_c^\top)$  (See Theorem 3), and  $H_c(\xi) = \log(\cosh(K\xi))^\top \mathbf{1}$ , where  $K \in \mathbb{R}^{3 \times 3}$  is chosen randomly. We discretize  $\Sigma_{pH}$  with the above parameters using the Itoh-Abe method [38] to obtain (16) and compare the results with the simple Forward Euler (FE). In both schemes, we chose a step size of  $h = 0.1$  seconds. The states and outputs of all controllers, i.e., continuous, discrete gradients, and FE, are plotted in Fig. 12 and Fig. 13, respectively. We observe that the trajectories of the continuous-time and discrete-time controllers using the Itoh-Abe method are nearly overlapping, whereas the trajectories of the controller based on FE method diverge. This comparison demonstrates the importance of using discrete-gradient methods for the discretization of dissipative controllers.

### E. Training of port-Hamiltonian controllers

One can solve the nonlinear OCP (7)-(8) by casting it as a NN training problem as follows [55],

$$\begin{aligned} \min_{\{\theta_k\}_{k=0}^L} & \frac{1}{S} \sum_{i=1}^S c(\mathbf{x}, \mathbf{u}; \theta_t, \mathbf{z}_0^k) \\ \text{s.t.} & \quad \mathbf{z}_0^i, \dots, \mathbf{z}_L^i = \text{ODESolve}\{f(\mathbf{z}_t, \theta_t, t), \mathbf{z}_0^i, (t_0, \dots, t_L)\}, \end{aligned}$$

where  $\theta_k$  are the samples of  $\theta_t$  at time steps  $(t_0, \dots, t_L)$ ,  $\mathbf{z}_i = [\mathbf{x}_i, \xi_i]$  are stacked states of the distributed system and the controller. Moreover, ODEsolve is any numerical solver

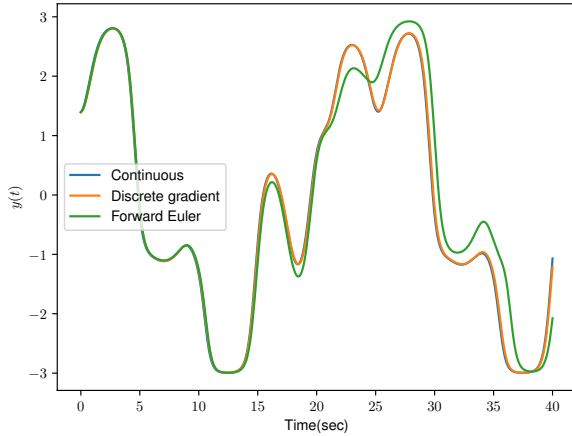


Fig. 13: The comparison of the outputs of the pH controllers subject to a sinusoidal input  $u(t) = \sin(t)$ .

that returns the sampled closed-loop trajectory  $z_0^i, \dots, z_L^i$  of the closed-loop  $f(\cdot) := \Sigma_s \|_f \Sigma_{pH}$  starting from an initial condition  $z_0^i$ , and  $L$  is the number of sampled states. Several ODE solvers can be used to simulate the dynamics, such as Foward Euler, or Dopri5 [79]. Once the closed-loop trajectories are obtained, one can evaluate the loss function  $c$ , and leverage BPTT to update the parameters via algorithms like Stochastic Gradient Descent (SGD) or Adam [80]. For details on training procedures, we refer the interested reader to [55].

*Remark 8 (Computation of  $\alpha$  through BPTT):* During BPTT, the following procedure can be adopted to ensure that  $\Sigma_{pH}$  remains dissipative throughout the optimization process: Perform forward propagation through the closed-loop system  $f(\cdot)$  using the current value of  $\vartheta$ . Compute  $\alpha$  according to either Theorem 3 or 4 for a batch of given initial conditions, and then calculate the training loss. ii) update the parameters  $\vartheta$  via BPTT, and iii) Recompute  $\alpha$  using the updated parameters.

1) *Implementation details for Experiment VI-A:* We simulate the closed-loop using FE with  $h = 0.0625$  for a finite horizon of  $T = 5$  secs. We train our controller for 1000 epochs. Particularly, we chose Adam [80] as the optimizer with a learning rate of 0.01 for training.

2) *Implementation details for Experiment VI-B:* The closed-loop is simulated using FE with a step-size of  $h = 2.5e - 5$  for  $T = 0.5$  secs. We train our controller with 2500 epochs using the Adam optimizer [80] with a learning rate of  $5 \times 10^{-3}$ .

We highlight that discretization during training might lead to sub-optimality. However, it does not compromise the closed-loop stability guarantees from Theorem 1, and 2. This is because the  $\mathcal{L}_2$  ( $i\mathcal{L}_2$ ) gain of continuous-time system  $\Sigma_{pH}$  holds regardless of the weights, as long as  $\alpha$  is chosen as in Theorem 3, or 4.

## REFERENCES

[1] H. S. Witsenhausen, "A counterexample in stochastic optimum control," *SIAM Journal on Control*, vol. 6, no. 1, pp. 131–147, 1968.

[2] L. Lessard and S. Lall, "Quadratic invariance is necessary and sufficient for convexity," in *IEEE American Control Conference (ACC)*, 2011, pp. 5360–5362.

[3] L. Furieri, C. L. Galimberti, M. Zakwan, and G. Ferrari-Trecate, "Distributed neural network control with dependability guarantees: a compositional port-Hamiltonian approach," in *Learning for Dynamics and Control Conference*. PMLR, 2022, pp. 571–583.

[4] L. Brunke, M. Greeff, A. W. Hall, Z. Yuan, S. Zhou, J. Panerati, and A. P. Schoellig, "Safe learning in robotics: From learning-based control to safe reinforcement learning," *Annual Review of Control, Robotics, and Autonomous Systems*, vol. 5, pp. 411–444, 2022.

[5] H. Tsukamoto, S.-J. Chung, and J.-J. E. Slotine, "Contraction theory for nonlinear stability analysis and learning-based control: A tutorial overview," *Annual Reviews in Control*, vol. 52, pp. 135–169, 2021.

[6] C. Dawson, S. Gao, and C. Fan, "Safe control with learned certificates: A survey of neural Lyapunov, barrier, and contraction methods," *arXiv preprint arXiv:2202.11762*, 2022.

[7] L. Furieri, C. L. Galimberti, and G. Ferrari-Trecate, "Learning to boost the performance of stable nonlinear systems," *IEEE Open Journal of Control Systems*, pp. 1–16, 2024.

[8] M. Zakwan, L. Xu, and G. Ferrari-Trecate, "Neural exponential stabilization of control-affine nonlinear systems," *arXiv preprint arXiv:2403.17793*, 2024.

[9] T. X. Nghiem, J. Drgoňa, C. Jones, Z. Nagy, R. Schwan, B. Dey, A. Chakrabarty, S. Di Cairano, J. A. Paulson, A. Carron *et al.*, "Physics-informed machine learning for modeling and control of dynamical systems," *arXiv preprint arXiv:2306.13867*, 2023.

[10] G. I. Beintema, M. Schoukens, and R. Tóth, "Deep subspace encoders for nonlinear system identification," *Automatica*, vol. 156, p. 111210, 2023.

[11] M. Revay, R. Wang, and I. R. Manchester, "Recurrent equilibrium networks: Flexible dynamic models with guaranteed stability and robustness," *IEEE Transactions on Automatic Control*, 2023.

[12] M. Zakwan, L. Di Natale, B. Svetozarevic, P. Heer, C. N. Jones, and G. Ferrari-Trecate, "Physically consistent neural ODEs for learning multi-physics systems," *IFAC-PapersOnLine*, vol. 56, no. 2, pp. 5855–5860, 2023.

[13] L. Di Natale, M. Zakwan, P. Heer, G. Ferrari-Trecate, and C. N. Jones, "Simba: System identification methods leveraging backpropagation," *arXiv preprint arXiv:2311.13889*, 2023.

[14] L. Di Natale, M. Zakwan, B. Svetozarevic, P. Heer, G. Ferrari-Trecate, and C. N. Jones, "Stable linear subspace identification: A machine learning approach," *arXiv preprint arXiv:2311.03197*, 2023.

[15] T. Asikis, L. Böttcher, and N. Antulov-Fantulin, "Neural ordinary differential equation control of dynamics on graphs," *Physical Review Research*, vol. 4, no. 1, p. 013221, 2022.

[16] L. Böttcher, N. Antulov-Fantulin, and T. Asikis, "AI pontryagin or how artificial neural networks learn to control dynamical systems," *Nature communications*, vol. 13, no. 1, p. 333, 2022.

[17] L. Hewing, J. Kabzan, and M. N. Zeilinger, "Cautious model predictive control using gaussian process regression," *IEEE Transactions on Control Systems Technology*, vol. 28, no. 6, pp. 2736–2743, 2019.

[18] L. B. Armenio, E. Terzi, M. Farina, and R. Scattolini, "Model predictive control design for dynamical systems learned by echo state networks," *IEEE Control Systems Letters*, vol. 3, no. 4, pp. 1044–1049, 2019.

[19] F. Bonassi, M. Farina, J. Xie, and R. Scattolini, "On recurrent neural networks for learning-based control: recent results and ideas for future developments," *Journal of Process Control*, vol. 114, pp. 92–104, 2022.

[20] E. Terzi, F. Bonassi, M. Farina, and R. Scattolini, "Learning model predictive control with long short-term memory networks," *International Journal of Robust and Nonlinear Control*, vol. 31, no. 18, pp. 8877–8896, 2021.

[21] M. Zakwan, L. Xu, and G. Ferrari Trecate, "Robust classification using contractive Hamiltonian neural ODEs," *IEEE Control Systems Letters*, vol. 7, pp. 145–150, 2022.

[22] A. van der Schaft, *L2-Gain and Passivity Techniques in Nonlinear Control*, 3rd ed., ser. Communications and Control Engineering. Cham: Springer International Publishing, 2017.

[23] F. Yang and N. Matni, "Communication topology co-design in graph recurrent neural network based distributed control," *arXiv preprint arXiv:2104.13868*, 2021.

[24] E. Tolstaya, F. Gama, J. Paulos, G. Pappas, V. Kumar, and A. Ribeiro, "Learning decentralized controllers for robot swarms with graph neural networks," in *Conference on robot learning*. PMLR, 2020, pp. 671–682.

[25] A. Khan, E. Tolstaya, A. Ribeiro, and V. Kumar, "Graph policy gradients for large scale robot control," in *Conference on robot learning*. PMLR, 2020, pp. 823–834.

- [26] F. Gama and S. Sojoudi, "Graph neural networks for distributed linear-quadratic control," in *Learning for Dynamics and Control*. PMLR, 2021, pp. 111–124.
- [27] L. Brunke, M. Greeff, A. W. Hall, Z. Yuan, S. Zhou, J. Panerati, and A. P. Schoellig, "Safe learning in robotics: From learning-based control to safe reinforcement learning," *arXiv preprint arXiv:2108.06266*, 2021.
- [28] R. Cheng, G. Orosz, R. M. Murray, and J. W. Burdick, "End-to-end safe reinforcement learning through barrier functions for safety-critical continuous control tasks," in *Proceedings of the AAAI Conference on Artificial Intelligence*, vol. 33, no. 01, 2019, pp. 3387–3395.
- [29] F. Berkenkamp, M. Turchetta, A. P. Schoellig, and A. Krause, "Safe model-based reinforcement learning with stability guarantees," *Advances in Neural Information Processing Systems 30*, vol. 2, pp. 909–919, 2018.
- [30] S. M. Richards, F. Berkenkamp, and A. Krause, "The Lyapunov neural network: Adaptive stability certification for safe learning of dynamical systems," in *Conference on Robot Learning*. PMLR, 2018, pp. 466–476.
- [31] T. Koller, F. Berkenkamp, M. Turchetta, and A. Krause, "Learning-based model predictive control for safe exploration," in *2018 IEEE conference on decision and control (CDC)*. IEEE, 2018, pp. 6059–6066.
- [32] P. Pauli, J. Köhler, J. Berberich, A. Koch, and F. Allgöwer, "Offset-free setpoint tracking using neural network controllers," in *Learning for dynamics and control*. PMLR, 2021, pp. 992–1003.
- [33] S. Abdulkhader, H. Yin, P. Falco, and D. Kragic, "Learning deep energy shaping policies for stability-guaranteed manipulation," *IEEE Robotics and Automation Letters*, 2021.
- [34] T. Duong and N. Atanasov, "Hamiltonian-based neural ODE networks on the SE (3) manifold for dynamics learning and control," *arXiv preprint arXiv:2106.12782*, 2021.
- [35] D. Martinelli, C. L. Galimberti, I. R. Manchester, L. Furieri, and G. Ferrari-Trecate, "Unconstrained parametrization of dissipative and contracting neural ordinary differential equations," *arXiv preprint arXiv:2304.02976*, 2023.
- [36] L. Massai, D. Saccani, L. Furieri, and G. Ferrari-Trecate, "Unconstrained learning of networked nonlinear systems via free parametrization of stable interconnected operators," *arXiv preprint arXiv:2311.13967*, 2023.
- [37] S. Z. Khong and A. van der Schaft, "On the converse of the passivity and small-gain theorems for input–output maps," *Automatica*, vol. 97, pp. 58–63, 2018.
- [38] M. J. Ehrhardt, E. S. Riis, T. Ringholm, and C.-B. Schönlieb, "A geometric integration approach to smooth optimisation: Foundations of the discrete gradient method," *arXiv preprint arXiv:1805.06444*, 2018.
- [39] M. Zakwan and G. Ferrari-Trecate, "Neural distributed controllers with port-Hamiltonian structures," *arXiv preprint arXiv:2403.17785*, 2024.
- [40] D. Angeli, "A Lyapunov approach to incremental stability properties," *IEEE Transactions on Automatic Control*, vol. 47, no. 3, pp. 410–421, 2002.
- [41] G.-B. Stan and R. Sepulchre, "Analysis of interconnected oscillators by dissipativity theory," *IEEE Transactions on Automatic Control*, vol. 52, no. 2, pp. 256–270, 2007.
- [42] D. N. Tran, B. S. Rüffer, and C. M. Kellett, "Incremental stability properties for discrete-time systems," in *2016 IEEE 55th Conference on Decision and Control (CDC)*. IEEE, 2016, pp. 477–482.
- [43] R. Sepulchre, T. Chaffey, and F. Forni, "On the incremental form of dissipativity," *IFAC-PapersOnLine*, vol. 55, no. 30, pp. 290–294, 2022.
- [44] M. Arcak, C. Meissen, and A. Packard, *Networks of dissipative systems: compositional certification of stability, performance, and safety*. Springer, 2016.
- [45] C. Verhoeck, P. J. Koelewijn, S. Haesaert, and R. Tóth, "Convex incremental dissipativity analysis of nonlinear systems," *Automatica*, vol. 150, p. 110859, 2023.
- [46] C. L. Galimberti, L. Furieri, L. Xu, and G. Ferrari-Trecate, "Hamiltonian deep neural networks guaranteeing non-vanishing gradients by design," *IEEE Transactions on Automatic Control*, pp. 1–8, 2023, doi: 10.1109/TAC.2023.3239430.
- [47] M. Zakwan, M. d'Angelo, and G. Ferrari-Trecate, "Universal approximation property of Hamiltonian deep neural networks," *IEEE Control Systems Letters*, vol. 7, pp. 2689–2694, 2023.
- [48] B. Amos, L. Xu, and J. Z. Kolter, "Input convex neural networks," in *International Conference on Machine Learning*. PMLR, 2017, pp. 146–155.
- [49] K. He, X. Zhang, S. Ren, and J. Sun, "Deep residual learning for image recognition," in *Proceedings of the IEEE conference on computer vision and pattern recognition*, 2016, pp. 770–778.
- [50] J. Nocedal and S. J. Wright, *Numerical optimization*. Springer, 1999.
- [51] Y. Wang, W. Yin, and J. Zeng, "Global convergence of admm in nonconvex nonsmooth optimization," *Journal of Scientific Computing*, vol. 78, pp. 29–63, 2019.
- [52] B. Houska, J. Frasch, and M. Diehl, "An augmented Lagrangian based algorithm for distributed nonconvex optimization," *SIAM Journal on Optimization*, vol. 26, no. 2, pp. 1101–1127, 2016.
- [53] L. T. Biegler and V. M. Zavala, "Large-scale nonlinear programming using ipopt: An integrating framework for enterprise-wide dynamic optimization," *Computers & Chemical Engineering*, vol. 33, no. 3, pp. 575–582, 2009.
- [54] P. J. Werbos, "Backpropagation through time: what it does and how to do it," *Proceedings of the IEEE*, vol. 78, no. 10, pp. 1550–1560, 1990.
- [55] R. T. Q. Chen, Y. Rubanova, J. Bettencourt, and D. K. Duvenaud, "Neural ordinary differential equations," in *Advances in Neural Information Processing Systems*, S. Bengio, H. Wallach, H. Larochelle, K. Grauman, N. Cesa-Bianchi, and R. Garnett, Eds., vol. 31. Curran Associates, Inc., 2018.
- [56] S. Foucart and H. Rauhut, *A Mathematical Introduction to Compressive Sensing*, ser. Applied and Numerical Harmonic Analysis. Springer New York, 2013. [Online]. Available: <https://books.google.ch/books?id=zb28BAAAQBAJ>
- [57] A. Paszke, S. Gross, F. Massa, A. Lerer, J. Bradbury, G. Chanan, T. Killeen, Z. Lin, N. Gimelshein, L. Antiga, A. Desmaison, A. Kopf, E. Yang, Z. DeVito, M. Raison, A. Tejani, S. Chilamkurthy, B. Steiner, L. Fang, J. Bai, and S. Chintala, "Pytorch: An imperative style, high-performance deep learning library," in *Advances in Neural Information Processing Systems 32*, 2019, pp. 8024–8035.
- [58] M. Xia, P. J. Antsaklis, and V. Gupta, "Passivity indices and passivation of systems with application to systems with input/output delay," in *53rd IEEE Conference on Decision and Control*. IEEE, 2014, pp. 783–788.
- [59] Y. Joo, R. Harvey, and Z. Qu, "Preserving and achieving passivity-short property through discretization," *IEEE Transactions on Automatic Control*, vol. 65, no. 10, pp. 4265–4272, 2019.
- [60] A. Martinelli, A. Aboudonia, and J. Lygeros, "Interconnection of discrete-time dissipative systems," *arXiv preprint arXiv:2311.08088*, 2023.
- [61] E. Hairer, M. Hochbruck, A. Iserles, and C. Lubich, "Geometric numerical integration," *Oberwolfach Reports*, vol. 3, no. 1, pp. 805–882, 2006.
- [62] O. Gonzalez, "Time integration and discrete Hamiltonian systems," *Journal of Nonlinear Science*, vol. 6, pp. 449–467, 1996.
- [63] A. Harten, P. D. Lax, and B. v. Leer, "On upstream differencing and godunov-type schemes for hyperbolic conservation laws," *SIAM review*, vol. 25, no. 1, pp. 35–61, 1983.
- [64] T. Itoh and K. Abe, "Hamiltonian-conserving discrete canonical equations based on variational difference quotients," *Journal of Computational Physics*, vol. 76, no. 1, pp. 85–102, 1988.
- [65] A. Macchelli, "Control design for a class of discrete-time Port-Hamiltonian systems," *IEEE Transactions on Automatic Control*, 2023.
- [66] S. Jafarpour, A. Davydov, A. Proskurnikov, and F. Bullo, "Robust implicit networks via non-euclidean contractions," *Advances in Neural Information Processing Systems*, vol. 34, pp. 9857–9868, 2021.
- [67] K. D. Smith, F. Seccamonte, A. Swami, and F. Bullo, "Physics-informed implicit representations of equilibrium network flows," *Advances in Neural Information Processing Systems*, vol. 35, pp. 7211–7221, 2022.
- [68] S. Jafarpour, M. Abate, A. Davydov, F. Bullo, and S. Coogan, "Robustness certificates for implicit neural networks: A mixed monotone contractive approach," in *Learning for Dynamics and Control Conference*. PMLR, 2022, pp. 917–930.
- [69] E. Winston and J. Z. Kolter, "Monotone operator equilibrium networks," *Advances in neural information processing systems*, vol. 33, pp. 10718–10728, 2020.
- [70] A. Moreschini, M. Mattioni, S. Monaco, and D. Normand-Cyrot, "Stabilization of discrete port-Hamiltonian dynamics via interconnection and damping assignment," *IEEE Control Systems Letters*, vol. 5, no. 1, pp. 103–108, 2020.
- [71] A. Tsolakis and T. Keviczky, "Distributed IDA-PBC for a class of non-holonomic mechanical systems," *IFAC-PapersOnLine*, vol. 54, no. 14, pp. 275–280, 2021.
- [72] J. Gimenez, C. Rosales, and R. Carelli, "Port-Hamiltonian modelling of a differential drive mobile robot with reference velocities as inputs," in *2015 XVI Workshop on Information Processing and Control (RPIC)*. IEEE, 2015, pp. 1–6.
- [73] P. Nahata, M. S. Turan, and G. Ferrari-Trecate, "Consensus-based current sharing and voltage balancing in DC microgrids with exponential loads," *IEEE Transactions on Control Systems Technology*, vol. 30, no. 4, pp. 1668–1680, 2021.

- [74] V. Otten *et al.*, “Power sharing in DC microgrids,” Ph.D. dissertation, 2020.
- [75] F. Strehle, M. Pfeifer, A. J. Malan, S. Krebs, and S. Hohmann, “A scalable port-Hamiltonian approach to plug-and-play voltage stabilization in DC microgrids,” in *2020 IEEE Conference on Control Technology and Applications (CCTA)*. IEEE, 2020, pp. 787–794.
- [76] E. D. Sontag and Y. Wang, “Notions of input to output stability,” *Systems & Control Letters*, vol. 38, no. 4-5, pp. 235–248, 1999.
- [77] L. Meng, Q. Shafiee, G. F. Trecate, H. Karimi, D. Fulwani, X. Lu, and J. M. Guerrero, “Review on control of DC microgrids and multiple microgrid clusters,” *IEEE journal of emerging and selected topics in power electronics*, vol. 5, no. 3, pp. 928–948, 2017.
- [78] A. van der Schaft and D. Jeltsema, “Port-Hamiltonian systems theory: An introductory overview,” *Foundations and Trends in Systems and Control*, vol. 1, no. 2-3, pp. 173–378, 2014.
- [79] M. Poli, S. Massaroli, A. Yamashita, H. Asama, and J. Park, “Torchdyn: A neural differential equations library,” *arXiv preprint arXiv:2009.09346*, 2020.
- [80] D. P. Kingma and J. L. Ba, “Adam: A method for stochastic gradient descent,” in *ICLR: International Conference on Learning Representations*, 2015, pp. 1–15.



**Muhammad Zakwan** is a doctoral assistant in the Dependable Control and Decision group (DE-CODE) at École Polytechnique Fédérale de Lausanne (EPFL). He is also a member of the National Centre of Competence in Research (NCCR) Automation. He holds an Electrical and Electronics Engineering degree from Bilkent University (Turkey) and a Bachelor of Science in Electrical Engineering from the Pakistan Institute of Engineering and Applied Sciences (Pakistan). His research interests include neural networks, nonlinear control, contraction

theory, port-Hamiltonian systems, and machine learning.



**Giancarlo Ferrari Trecate** (SM'12) received a Ph.D. in Electronic and Computer Engineering from the Università Degli Studi di Pavia in 1999. Since September 2016, he has been a Professor at EPFL, Lausanne, Switzerland. In the spring of 1998, he was a Visiting Researcher at the Neural Computing Research Group, University of Birmingham, UK. In the fall of 1998, he joined the Automatic Control Laboratory, ETH, Zurich, Switzerland, as a Postdoctoral Fellow. He was appointed Oberassistent at ETH in 2000. In 2002, he joined INRIA, Rocquencourt,

France, as a Research Fellow. From March to October 2005, he was a researcher at the Politecnico di Milano, Italy. From 2005 to August 2016, he was Associate Professor at the Dipartimento di Ingegneria Industriale e dell'Informazione of the Università degli Studi di Pavia. His research interests include scalable control, machine learning, microgrids, networked control systems, and hybrid systems. Giancarlo Ferrari Trecate is the founder and current chair of the Swiss chapter of the IEEE Control Systems Society. He is Senior Editor of the IEEE Transactions on Control Systems Technology and has served on the editorial boards of *Automatica* and *Nonlinear Analysis: Hybrid Systems*.